Chem Soc Rev

REVIEW ARTICLE

View Article Online
View Journal | View Issue

Open Access Article. Published on 08 august 2016. Downloaded on 21.04.2026 03:42:46.
This article is licensed under a Creative Commons Attribution 3.0 Unported Licence.

Cite this: *Chem. Soc. Rev.*, 2016, 45, 6327

Applications of N-heterocyclic imines in main group chemistry

Tatsumi Ochiai,[a] Daniel Franz[b] and Shigeyoshi Inoue*[ab]

Received 29th February 2016

DOI: 10.1039/c6cs00163g

www.rsc.org/chemsocrev

The imidazolin-2-imino group is an N-heterocyclic imino functionality that derives from the class of compounds known as guanidines. The exocyclic nitrogen atom preferably bonds to electrophiles and its electron-donating character is markedly enhanced by efficient delocalization of cationic charge density into the five-membered imidazoline ring. Thus, this imino group is an excellent choice for thermodynamic stabilization of electron-deficient species. Due to the variety of available imidazoline-based precursors to this ligand, its steric demand can be tailored to meet the requirements for kinetic stabilization of otherwise highly reactive species. Consequently, it does not come as a surprise that the imidazolin-2-iminato ligand has found widespread applications in transition-metal chemistry to furnish pincer complexes or "pogo stick" type compounds. In comparison, the field of main-group metal compounds of this ligand is still in its infancy; however, it has received growing attention in recent years. A considerable number of electron-poor main-group element species have been described today which are stabilized by N-heterocyclic iminato ligands. These include low-valent metal cations and species that are marked by formerly unknown bonding modes. In this article we provide an overview on the present chemistry of main-group element compounds of the imidazolin-2-iminato ligand, as well as selected examples for the related imidazolidin- and benzimidazolin-2-imino system.

Introduction

The imidazolin-2-imino group is a potent electron pair donor

In coordination chemistry nitrogen is particularly recognized for its role as a strong electron-donor atom in ligand systems. Seemingly, this contradicts the fact that this element belongs to the highly electronegative members of the periodic table.

[a] *Institut für Chemie, Technische Universität Berlin, Straße des 17. Juni 135, 10623 Berlin, Germany. E-mail: s.inoue@tum.de*
[b] *Department of Chemistry, Institute of Silicon Chemistry and Catalysis Research Center, Technische Universität München, Lichtenbergstraße 4, 85748 Garching, Germany*

Tatsumi Ochiai

Tatsumi Ochiai was born in Shizuoka, Japan, in 1987. In 2012 he received his MSc degree from the University of Tsukuba under the supervision of Prof. Akira Sekiguchi, for which he received the Dean's Prize. He worked on heteroatom-substituted tetrahedranes. He then moved to Berlin in 2012 starting doctoral work in the research group of Prof. Shigeyoshi Inoue. His research interest mainly focuses on the synthesis of low-coordinate heavier group 14 elements, metallylenes and metallyliumylidene ions.

Daniel Franz

Daniel Franz studied chemistry at the Goethe University Frankfurt am Main, Germany, where he received his PhD degree under the supervision of Prof. Matthias Wagner in 2012. Following this he moved to Berlin to carry out postdoctoral studies in the group of Prof. Shigeyoshi Inoue. Today he is pursuing his research interests in coordination chemistry of group 13 and 14 elements at the Technische Universität München under the supervision of Prof. Inoue.

Open Access Article. Published on 08 august 2016. Downloaded on 21.04.2026 03:42:46.
This article is licensed under a Creative Commons Attribution 3.0 Unported Licence.

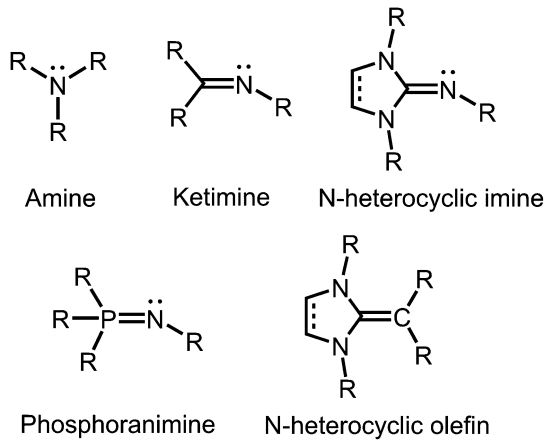

Fig. 1 Overview of selected N-donor ligands and the related N-heterocyclic olefin (R = organyl or H).

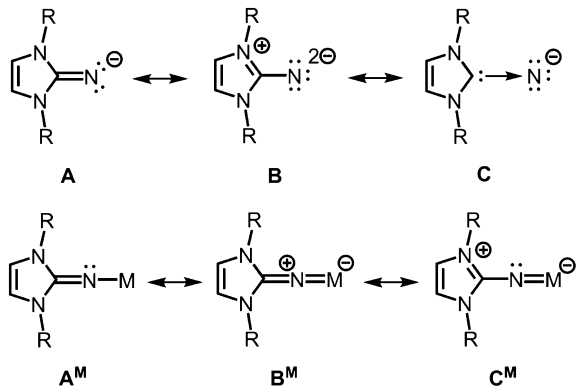

Fig. 2 Selected resonance structures for the anionic imidazolin-2-iminato ligand, as well as a model complex with M^+ (R = organyl).

However, the trivalent nitrogen atom in amines, as well as in imines has high electron density in the form of a lone pair that it readily shares with various types of hard and soft Lewis acids.

Tertiary amines and secondary ketimines resemble in their nucleophilic properties but, in sharp contrast, the unsaturated carbon atom of the imino functionality is prone to the reaction with nucleophiles or reducing agents whereas the amino carbon atom is inert (Fig. 1). This reactivity results from the π-interaction with the more electronegative nitrogen atom which provides the higher bond order but also drains electron density from the carbon centre in the σ-, as well as the π-scaffold. Due to the orthogonal orientation of the nitrogen lone pair this is not compensated by π back donation. Interestingly, the electronic properties of the imino-nitrogen atom are, *vice versa*, stronger affected by the characteristics of the carbon atom than it may be the case for the amino-nitrogen centre. In this regard, the electron-rich π-system of an imidazoline ring not only mitigates the electrophilicity of an imino-carbon atom incorporated at the 2-position of the cycle but also pushes electron density to the exocyclic imino-nitrogen atom (Fig. 1). Notably, phosphoranimines ($R_3P{=}NR$) resemble the imidazolin-2-imines in the electron-donating character of the imino nitrogen atom (Fig. 1). The resemblance of these two ligand classes is reasoned by the similarities in the electronic properties of the parent phosphine and imidazolin-2-ylidene, respectively. Furthermore, one must recognize the isoelectronic relation between imidazolin-2-imines and N-heterocyclic olefins, which function as strong Lewis bases due to the ylide-like nature of the exocyclic alkene bond (Fig. 1).[1]

The allocation of electron density from the five-membered imidazoline ring to the exocyclic nitrogen atom is illustrated by conceivable resonance structures of the anionic imidazolin-2-iminato ligand **A** (Fig. 2).[2,3] The canonical form **B** in which the exocyclic nitrogen atom bears two formal anionic charges suggests a significant boost of its electron-donating properties as compared to ketimines (Fig. 1 and 2). Form **C** represents the partial N-heterocyclic carbene (NHC) character of the imidazoline moiety (Fig. 2). As apparent from the canonical forms (**A–C**) the imidazolin-2-iminato ligand represents a 2σ electron donor with potential to contribute an additional two or even four π-electrons. Consequently, its metal complexes ($\mathbf{A^M}$) may exhibit significant metalla-2-aza-allene ($\mathbf{B^M}$) or metalimide ($\mathbf{C^M}$) character (Fig. 2). This manifests in an expansion of the imino group's CN distance and shortening of the N–M bond length. Concomitantly, the C–N–M bond angle is widened to approach the angle of 180° in the ideal CCC allene structure motive. As a result of its electron-donating properties, the imidazolin-2-iminato ligand is an efficient tool for the thermodynamic stabilization of electron-poor species. Moreover, the bulkiness of the imidazoline ring can be conveniently modified to meet individual requirements for kinetic stabilization of otherwise elusive compounds.

Shigeyoshi Inoue

Shigeyoshi Inoue studied chemistry at the University of Tsukuba where he completed his PhD degree under the supervision of Prof. Akira Sekiguchi in 2008. After being a Humboldt Postdoctoral fellow, as well as a JSPS postdoctoral fellow for research abroad with Prof. Matthias Drieß at the Technische Universität Berlin, he began his independent research career as a Sofia Kovalevskaja Professor in 2010 at the same university. Since 2015 he has been a W2-Tenure-Track Professor of Silicon Chemistry at the Technische Universität München. His research interests are focused on the synthesis and reactivity investigation of low-valent main group compounds with the goal of finding novel applications in synthesis and catalysis.

The scope of this review

In this article we focus on the coordination chemistry of the imidazolin-2-iminato ligand, as well as the strongly related imidazolidin-2-imino group and the benzimidazolin-2-imino group with regard to main-group elements. For the latter two

 This journal is © The Royal Society of Chemistry 2016

Open Access Article. Published on 08 august 2016. Downloaded on 21.04.2026 03:42:46.
This article is licensed under a Creative Commons Attribution 3.0 Unported Licence.

only relevant examples will be given. An earlier review of Kuhn, Frenking and coworkers on imidazolin-2-imines includes main-group metal complexes but dates back about 13 years.[2] The broad spectrum of transition metal complexes that comprise this ligand class and the methods for the synthesis of the ligand have recently been reviewed by Tamm and coworkers and will be discussed only in part.[3]

Moreover, only selected examples will be discussed for compounds of this iminato ligand with the non-metals carbon and nitrogen because this belongs to the field of organic chemistry rather than coordination chemistry.

Group 1 and group 2 element complexes

Background

About 20 years ago Kuhn and coworkers started their pioneering studies on the chemistry of imidazolin-2-imines.[4] A few alkaline[5,6] and alkaline earth[7] compounds of the imino group were reported but not investigated thoroughly probably because of the pronounced polar nature of the N–M bond (M = alkaline or alkaline earth metal). This puts them in the role of a reactive intermediate for ligand transfer *via* salt metathesis rather than a species with its own follow-up reactivity with sustainment of the N–M bond. Accordingly, the chemistry of group 1 and group 2 imidazolin-2-iminato complexes is only explored to a minor degree to date.

Lithium and potassium complexes

The reaction of $L^{Me_2}NH$ (L^{Me_2} = 1,3-dimethyl-imidazolin-2-ylidene) with MeLi in Et_2O produces $L^{Me_2}NLi$ (**1**) which is the N-lithiated derivative of the imidazolin-2-imine.[5] The species was characterized by ^1H NMR analysis and according to the reported CHN elemental analysis no solvent was present in the isolated material. If the conversion was carried out in THF/Et_2O with MeLi that was prepared from H_3CCl and elemental lithium without prior separation of lithium chloride, crystals of the unexpected composition $[Li_{12}O_2Cl_2(L^{Me_2}N)_8(thf)_4]\cdot 8THF$ (**2**) were retrieved in low yield (Scheme 1).

The solid state structure of **2** is marked by a $Li_{12}N_8O_2Cl_2$ cage that comprises a peroxo moiety in its core (Fig. 3). The authors

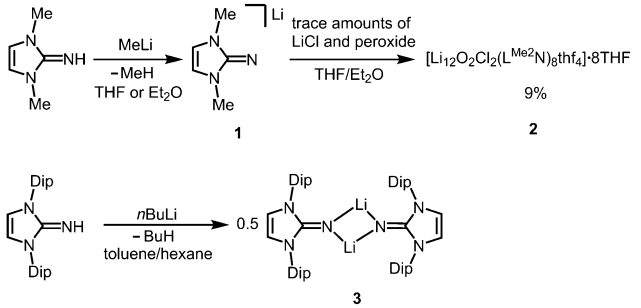

Scheme 1 Conversion of the imino lithium species **1** into the imino-stabilized LiOCl aggregate **2** (the lithium chloride derives from the methyllithium synthesis and peroxide from contaminated solvent). Formation of the bulky imino lithium dimer **3** (Dip = 2,6-diisopropylphenyl).

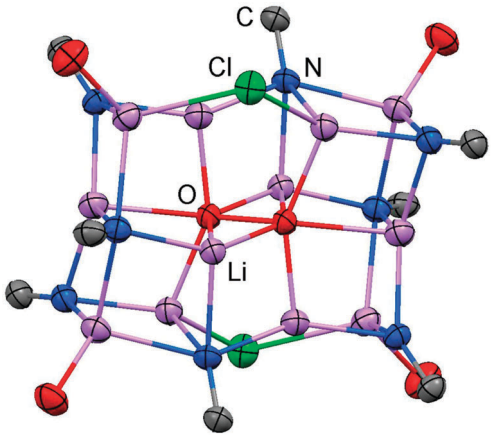

Fig. 3 Ellipsoid plot (30% level) of the $Li_{12}N_8O_2Cl_2$ cage in **2** with adjacent imino-carbon atoms and oxygen atoms of coordinated THF.

reasoned that the O_2^{2-} group resulted from contamination of the solvent with traces of peroxide. Crystals of dimeric $[L^{Dip}NLi]_2$·toluene (**3**·toluene, L^{Dip} = 1,3-bis(2,6-diisopropylphenyl)-imidazolin-2-ylidene) were isolated in good yield after the reaction of $L^{Dip}NH$ with *n*BuLi in toluene/hexane.[8] Apparently, the formation of higher aggregates is hampered by the bulkier Dip groups (Dip = 2,6-diisopropylphenyl). Bringing into contact $L^{Me_2}NH$ and freshly prepared MeK in Et_2O afforded the heavier alkaline derivative $L^{Me_2}NK$ (**4**).[6] The compound was characterized by elemental analysis and its existence was verified by the synthesis of the dithiocarbiminate $L^{Me_2}NCS_2K$ (**5**, Scheme 2). Interestingly, the latter shows structural characteristics that account for a bonding situation as represented by resonance structure $\mathbf{5^B}$ (Scheme 2) with the C–N_{imino} bond length significantly increased (a range from 1.369(16) Å to 1.379(18) Å is observed in the solid state structure; *cf.* **2**: C–N_{imino} = 1.260(4)–1.263(4) Å; **3**: C–N_{imino} = 1.241(3) Å, 1.242(4) Å). Accordingly, the C–S distances in **5** (1.733(13)–1.755(13) Å) resemble typical CS single bond lengths.

Magnesium complexes

As rare examples for N-heterocyclic iminato complexes of group 2 metals the magnesium compounds $(L^{Me_2}NH)_4MgI_2$ ($\mathbf{6}[I]_2$), as well as $\{L^{Me_2}NMgI\}_n$ (**7**) and $\{(L^{Me_2}N)_2Mg\}_n$ (**8**), were reported by Kuhn and coworkers ($n \geq 1$).[7] They are accessed through $L^{Me_2}NH$ *via* conversion with 0.25 MgI_2, MeMgI and $(n\text{Bu})_2Mg$, respectively (Scheme 3). Single crystal XRD (X-ray diffraction) data were obtained for $\mathbf{6}[I]_2$ (Fig. 4) while the degree of aggregation (n) of **7** and **8** was not elucidated by structural analysis.

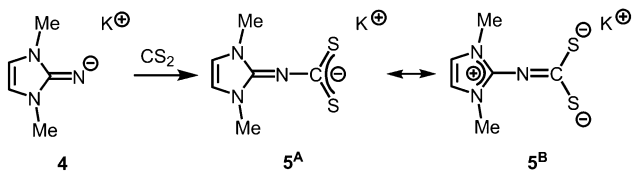

Scheme 2 Conversion of potassium imide **4** with carbon disulfide to the thiocarbiminate **5** (represented by resonance structures $\mathbf{5^A}$ and $\mathbf{5^B}$).

Open Access Article. Published on 08 august 2016. Downloaded on 21.04.2026 03:42:46.
This article is licensed under a Creative Commons Attribution 3.0 Unported Licence.

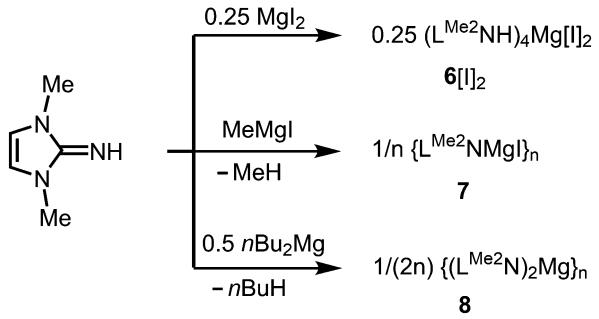

Scheme 3 Synthesis of the imino-magnesium compounds **6**$[I]_2$, **7** and **8**.

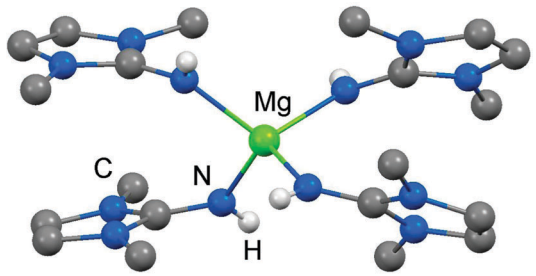

Fig. 4 Ball and stick representation of $(L^{Me_2}NH)_4Mg^{2+}$ (**6**$^{2+}$) as derived from XRD analysis (non-N-bonded hydrogen atoms have been omitted).

Notably, **6**$[I]_2$ also formed if less than four equiv. of the imine were reacted with MgI_2. The authors attributed this observation to the high basicity of the ligand.

Group 13 element complexes

Background

Of group 13 elements only a few aluminium complexes with an N-heterocyclic iminato ligand had been reported until respective research was resumed by our group.[6] Reports[8–10] in the year 2014 were the first to describe imidazolin-2-imino complexes of boron. In contrast, the coordination chemistry of related phosphoranimines of boron[11] and aluminium[11a,c,d,12] is thoroughly studied.

Boron complexes

The Lewis acid base adducts $LNH(BH_3)$ (**9**, Scheme 4) between $L^{Dip}NH$, as well as $L^{Mes}NH$ (L^{Mes} = 1,3-dimesityl-imidazolin-2-ylidene), and the parent borane were isolated after conversion of the imine with $Me_2S{\cdot}BH_3$ in toluene.[9] When treated with imidazolin-2-ylidenes (L) dihydrogen is abstracted from the HN–BH moiety of these imine–borane compounds and along with $L(H_2)$ (hydrogenated at the formerly carbenic centre) the NHC-adducts of respective imino boron dihydrides ($LN(BH_2)L$) are formed (**10**, Scheme 4).[9] These NHC-adducts undergo hydride-mediated ring-expansion reaction, that is, the boron atom transfers its two hydrides to the adjacent carbon atom and inserts into the $C_{carbenoid}N$ bond of the NHC (**11**, Scheme 4).[9] Presumably, the interaction between the lone pair at the imino nitrogen atom and the unoccupied p-orbital at the boron centre

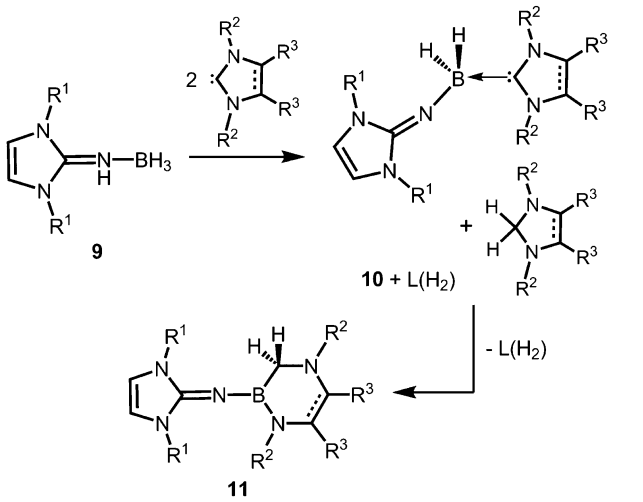

Scheme 4 Conversion of the imine–borane adduct **9** with NHC to iminoboron dihydride NHC complex **10** and the formation of **11** *via* ring expansion reaction. R^1 = Mes or Dip; R^2 = Me (for R^3 = Me), Mes or Dip (both for R^3 = H); R^2 = Mes and R^3 = H for unsaturated backbone; not all combinations of imine and NHC are viable for **10** and **11**.[9]

supports the trigonalization of the metalloid atom. Interestingly, this insertion occurs at higher temperatures with more sterically hindered substituents at the boron atom. Moreover, H_2L^{Mes} (1,3-dimesityl-imidazolidin-2-ylidene, NHC saturated at the ligand backbone) is subject to ring-expansion reaction at significantly lower temperatures than its congener of very similar sterical encumbrance L^{Mes} (NHC unsaturated at the ligand backbone). It was reasoned that the conjugated ring system in L^{Mes} is more efficient for the delocalization of positive charge density and, thus, stabilizes the boron dihydride form ($LNBH_2L$).

Similarly, ring-activation and expansion reaction of L^{Dip} took place by heating the amido-substituted hydridoborane $L^{Dip}(BH_2)HNDip$ reported by Rivard and coworkers.[13]

Conversion of the bis(iminiumtosylate) **12**$[OTs]_2$ with $Li[BH_4]$ furnishes the boronium salt **13**[OTs] (Scheme 5).[10] The compound reacts with yellow sulfur to give a rare example of a cationic thioxoborane **14**[OTs] that was structurally characterized (Scheme 5).[10] The B–S bond length (1.710(5) Å) in **14**$^+$ is the shortest that has been reported to date for a molecular complex. Notably, the B–N bond lengths significantly decrease upon transformation of tetrahedral **13**$^+$ into trigonal-planar **14**$^+$ (**13**$^+$: 1.573(5) Å, 1.577(5) Å; **14**$^+$: 1.483(5) Å, 1.493(5) Å) and, consequently, a partial double bond character can be attributed to the boron–nitrogen interactions in **14**$^+$. Concomitantly, the C–N distances of the imino groups increase (**13**$^+$: 1.317(5) Å, 1.318(4) Å; **14**$^+$: 1.359(4) Å, 1.363(4) Å) which is in accordance with the formulation of resonance structure **14**$^{A+}$ (Scheme 5) that represents the delocalization of positive charge density into the N-heterocycles and the polarization of the BS bond towards the sulfur atom (NBO charge at S = −0.58; NBO = Natural Bond Orbital). DFT (density functional theory) calculations supported the interpretation of the remarkably short B–S distance in terms of a boron sulfur double bond. For example, the HOMO (highest occupied molecular orbital) shows mainly

 This journal is © The Royal Society of Chemistry 2016

Open Access Article. Published on 08 august 2016. Downloaded on 21.04.2026 03:42:46.
This article is licensed under a Creative Commons Attribution 3.0 Unported Licence.

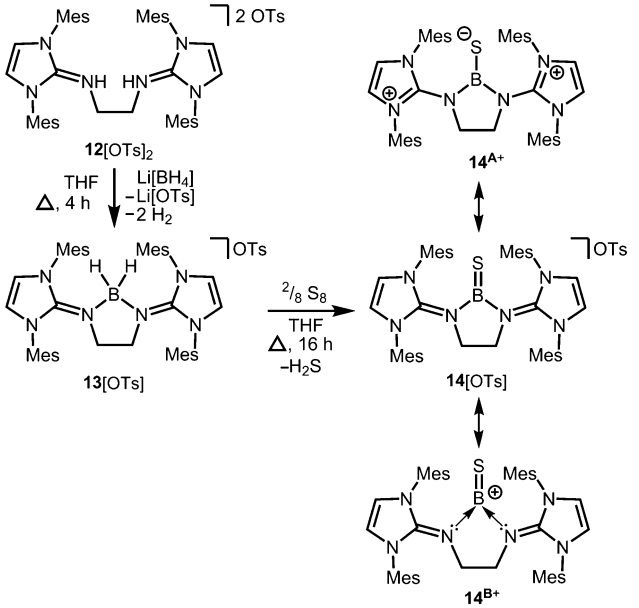

Scheme 5 Reaction of the bis(iminiumtosylate) **12**$[OTs]_2$ with lithium borohydride to the boronium salt **13**[OTs] (Ts = tosyl) and its conversion to the thioxoborane salt **14**[OTs].

the sulfur lone pair and the HOMO−1 reveals the B=S π-bonding orbital. The NBO charge at the boron centre of $\mathbf{14}^+$ was calculated to be +0.63 which accounts for the boron cation character of the complex as illustrated by the canonical form $\mathbf{14}^{\mathbf{B}+}$ (Scheme 5).

Very recently, Rivard and coworkers described the conversion of the imidazolin-2-imino trimethylsilane **15** to the imino boron dichloride **16** and its organyl derivative **17** by the reaction of **15** with BCl_3 and $PhBCl_2$, respectively (Scheme 6).[14] The bisimino boron monochloride **18** was furnished in a reaction between **15** and **16** (Scheme 6). Moreover, the synthesis of the diphenyl congener **19** was accomplished by conversion of **17** with phenylmagnesium bromide (Scheme 6). The solid state structure of the dihalide **16** hints toward the significant bora-2-aza-allene properties of the CNB moiety (type $\mathbf{B}^{\mathbf{M}}$, Fig. 2) as concluded from the C–N–B bond angle of 180° and the short B–N bond length (1.302(6) Å) which implies high boron–nitrogen double bond character. Remarkably, **16**, **17** and **19** react with amine–boranes ($R_nH_{3-n}N{\cdot}BH_3$; R = H, Me; n = 1, 2) to produce the respective dihydrogenated imino boron compounds $L^{Dip}NH(B(H)R'R'')$ **20–22** (R′ = R″ = Cl for **20**; R′ = Cl, R″ = Ph for **21**; R′ = R″ = Ph for **22**) and a mixture of the amine–borane dehydrogenation products (Scheme 6).[14] The authors conclude that this imino boron compound acts as an intramolecular frustrated Lewis acid base pair. It should be noted that compound **17** displays catalytic activity in the dehydrocoupling of $MeNH_2{\cdot}BH_3$ to yield $[MeNBH]_3$ along with oligomeric aminoboranes, which shows its great potential with respect to further application in metal-free catalysis for the dehydrocoupling of amine–boranes and related species.

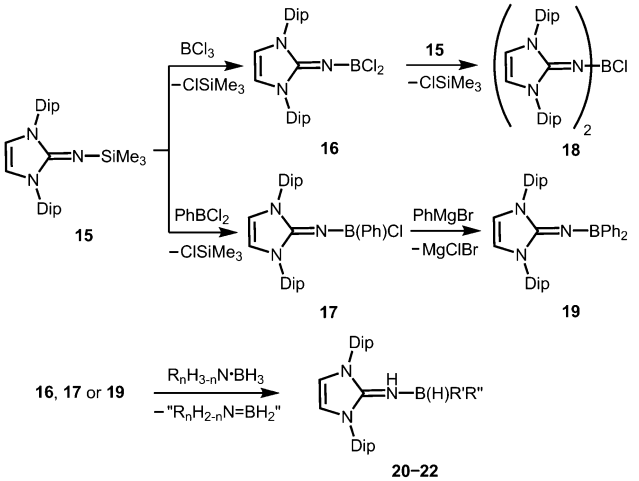

Scheme 6 Conversion of the imino trimethylsilane **15** to the imino chloroboranes **16–18** and the imino diphenylborane **19**. Formation of the imine–borane adducts *via* abstraction of dihydrogen from amine–borane adducts.

Aluminium complexes

The bisimino aluminium complexes $(L^{Me_2}NSiMe_3)_2AlMe_2[Cl]$ (**23**) and $(L^{Me_2}NH)_2AlMe_2[Cl]$ (**24**) were synthesized by conversion of $L^{Me_2}NSiMe_3$ (**25**) and $L^{Me_2}NH$, respectively, with 0.5 equiv. of $AlMe_2Cl$.[7] The ion-separated forms were postulated on the basis of NMR spectroscopic data. The related Lewis acid base adduct $L^{Me_2}NSiMe_3{\cdot}AlCl_3$ (**26**) releases Me_3SiCl upon heating the neat compound to 180 °C and is converted into $\{L^{Me_2}NAlCl_2\}_3$ (**27**, Scheme 7).[7] An X-ray crystallographic analysis of compound **27** verified its trimeric structure with a six-membered Al_3N_3 cycle.

The imino aluminium dihydride $\{L^{Dip}NAlH_2\}_2$ (**28**) results from the reaction of $L^{Dip}NH$ with $Me_3N{\cdot}AlH_3$ (Scheme 7).[8] From the dihydride one can derive the dihalides $\{L^{Dip}NAlX_2\}_2$ (**29–31**, X = Cl, Br, I) by conversion with BX_3 (two equiv.) which were described to form dimers in the solid state, as well as in solution (Scheme 8).[7] Obviously, the bulkier iminato ligand in **29** leads to the formation of a four-membered Al_2N_2 ring with smaller N–Al–N angles (87.8(1)°, 92.3(1)°) in comparison to the six-membered ring in **27** with larger angles (108–110°). Interestingly, the sterically hindered phosphoranimino aluminium dihydride and -dichloride form dimers with four-membered Al_2N_2 rings

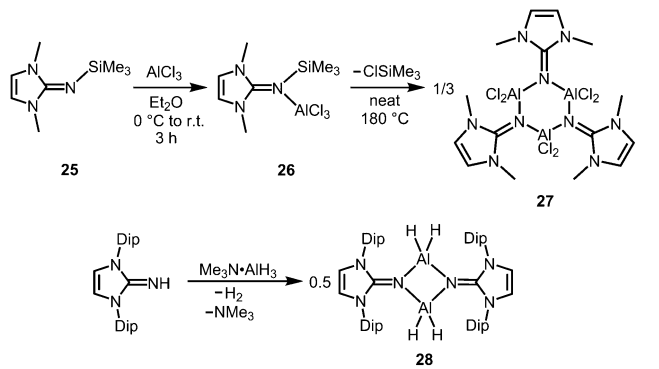

Scheme 7 Conversion of the trimethylsilylimine **25** to the aluminium trichloride imine complex **26** and its transformation into trimeric **27**.

Open Access Article. Published on 08 august 2016. Downloaded on 21.04.2026 03:42:46.
This article is licensed under a Creative Commons Attribution 3.0 Unported Licence.

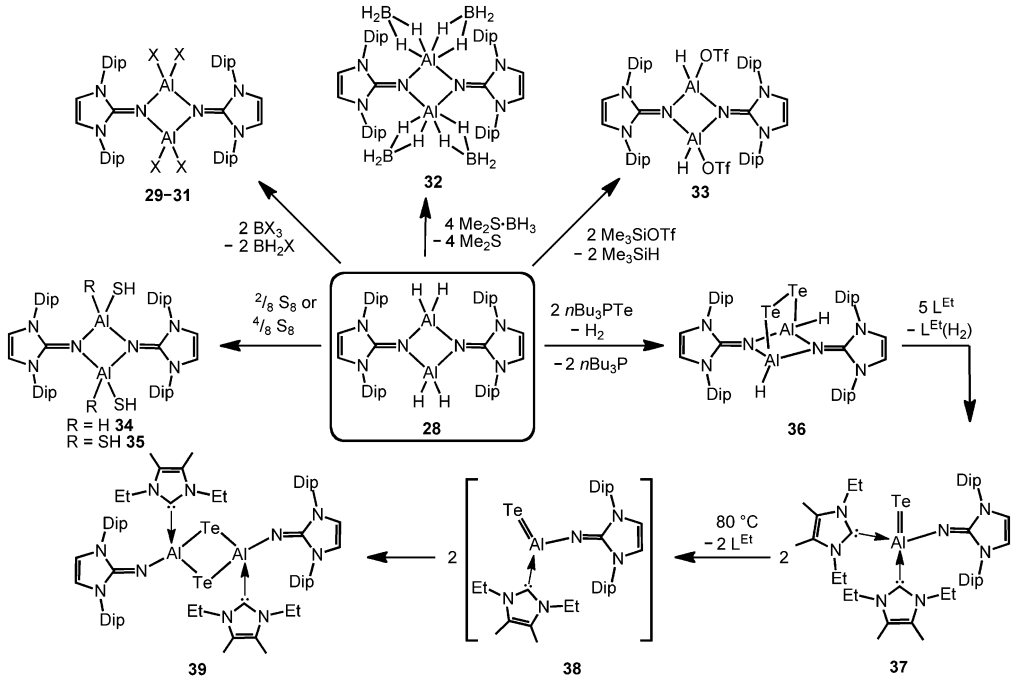

Scheme 8 Overview on syntheses of imino aluminium compounds derived from the aluminium dihydride **28**: reaction of **28** to the dihalides **29–31**, the borohydride **32** and the triflate **33** (X = Cl, Br, I). Synthesis of the aluminium mono- and bis(hydrogensulfides) **34**, as well as **35**. Conversion of **28** to the ditelluride **36** and its monotopic aluminium telluride offspring **37** (L^{Et} = 1,3-diethyl-4,5-dimethyl-imidazolin-2-ylidene). Transformation of **37** to ditopic **39** *via* the presumed intermediate **38**.

({R_3PNAlX_2}$_2$; R = iPr, *t*Bu; X = H, Cl), as well.[11c,12a] Furthermore, the dihydride **28** reacts with the electrophiles $Me_2S{\cdot}BH_3$ (four equiv.) and Me_3SiOTf (two equiv., Tf = triflyl) to yield the aluminum borohydride **32** and the aluminium monohydride triflate **33**, respectively (Scheme 8).[8] Notably, the substitution of both aluminium bonded hydrides in **33** for triflate substituents could not be accomplished by the use of a larger excess of Me_3SiOTf, even at elevated temperature. In contrast, the conversion of **28** with only two equiv. of $Me_2S{\cdot}BH_3$ does not afford the expected aluminium monohydride borohydride as a product but yields mixtures of **28** and **32**. Obviously, the electron withdrawing triflyl groups in **33** mitigate the hydride-donor strength of the remaining AlH functionality. Accordingly, only aluminium monohydride triflates of the related phosphoraniminato or the 1,3-diketiminato ligand have been reported.[11c,15] The conversion of the aluminium dihydride **28** with yellow sulfur affords a rare example of an aluminium hydride hydrogensulfide complex (**34**) by insertion of a sulfur atom into the AlH bond (Scheme 8).[16] Similar to **33** the remaining hydride functionalities at the aluminium centres in **34** are less reactive than in the parent compound. However, the transformation with S_8 to form the bis(hydrogensulfide) **35** can be forced onto the system by heating (90 °C for four days, Scheme 8).[16] As apparent from the XRD study the Al–S distances in **35** (2.231(1)–2.240(1) Å) are slightly shorter than the respective distances in the monohydrogensulfide **34** (2.250(1) Å and 2.252(1) Å).

In order to furnish a heavier aluminium chalcogenide of the imidazolin-2-iminato ligand, **28** was converted with the tellurium atom transfer reagent nBu_3PTe (two equiv.).[17] This conversion yields ditopic aluminium ditelluride **36** as a rare example of an electron-precise aluminium complex with the chalcogen in the oxidation state −1 (Scheme 8). The hydrides left at the aluminium centres in **36** do not react further with excess nBu_3PTe. However, the compound converts with NHC (L^{Et}, 5 equiv., L^{Et} = 1,3-diethyl-4,5-dimethyl-imidazolin-2-ylidene) in a dehydrogenative redox process to form the monotopic aluminium telluride **37** (Fig. 5, Scheme 8) with the chalcogen in the oxidation state −2 along with dihydrogenated NHC ($L^{Et}(H_2)$).[17]

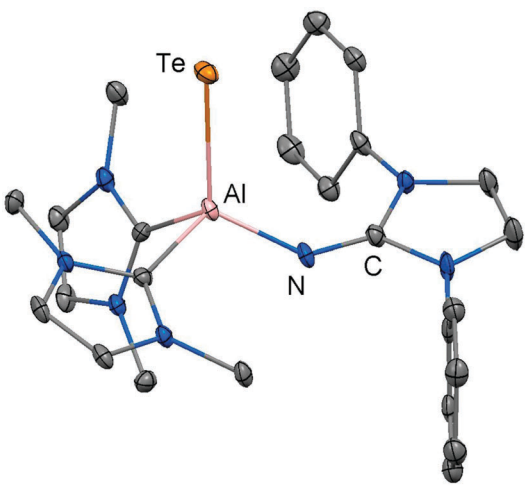

Fig. 5 Ellipsoid plot (30% level) of the aluminium telluride **37** (hydrogen atoms, isopropyl groups and non-N-bonded methyl groups have been omitted).

 This journal is © The Royal Society of Chemistry 2016

Open Access Article. Published on 08 august 2016. Downloaded on 21.04.2026 03:42:46.
This article is licensed under a Creative Commons Attribution 3.0 Unported Licence.

The structural study of **37** revealed a remarkably short Al–Te distance of 2.5130(14) Å and DFT calculations determined an enhanced aluminium–tellurium interaction (WBI_{AlTe} = 1.20; NPA charges: Al = +1.24, Te = −0.95; WBI = Wiberg bond index, NPA = natural population analysis). It has to be pointed out that the terminal position of the tellurium atom is a very scant structural motif as group 16 atoms commonly assume bridging positions in aluminium chalcogenides. Upon heating a benzene solution of **37** to 80 °C one of the two L^{Et} ligands is released and the putative intermediate $L^{Dip}N(AlTe)L^{Et}$ (**38**) undergoes aggregation to form **39** (Scheme 8).

The reaction pathway *via* **38** was suggested by DFT calculations; however, the isolation of a bulkier congener of this elusive species was not accomplished by the use of more sterically hindered NHC. The structural investigation of **39** revealed significantly increased Al–Te distances (2.6143(14) Å, 2.6211(15) Å) and a decreased bond order for the AlTe interaction (WBI_{AlTe} = 0.75; NPA charges: Al = +1.21, Te = −0.79) with respect to **37**.[17] It should be noted that in ditopic **39** the aluminium centres are bridged *via* the tellurium atoms. Notably, **37** and **39** contrast the other given examples for aluminium complexes of the imidazolin-2-iminato ligand in that the aluminium centres are not connected *via* the nitrogen atoms of the imino groups. Taking into account the marked changes in the Al–Te distances and the values for the WBI_{AlTe} upon transformation of **37** into **39** the nature of the AlTe interaction in **37** was presumed to possess high Al═Te double bond character.

Group 14 element complexes

Background

In initial reports on the chemistry of N-heterocyclic iminato ligands Kuhn and coworkers described the imino trimethylsilane **25** (Scheme 7) which was used as an alternative transmetallation reagent to the alkaline metal salts mentioned above.[4,7] Presumably, the bulkier $L^{Mes}NSiMe_3$ is formed as an intermediate in the synthesis of $L^{Mes}NH$ *via* a Staudinger-type reaction described by Cameron, Jenkins, Clyburne and coworkers in 2001.[18] Tamm and coworkers established the general method for the preparation of trimethylsilyl-functionalized bulkier imidazolin-2-iminato ligands such as $L^{Mes}NSiMe_3$ and $L^{Dip}NSiMe_3$ in 2004.[19] This method has tremendous advantages for the convenient and high-yield synthesis of various imidazolin-2-imines. Moreover, a silicon atom was incorporated into the spacer group between the imino- and the arene moiety in oligodentate ligands reported by Tamm and coworkers.[20] However, it played a rather passive role in the chemistry of the transition metal complexes derived from this ligand system. As outlined in the following section a considerable time elapsed from Kuhn's initial report until the coordination chemistry of the imidazolin-2-iminato ligand with tetrel atoms was thoroughly investigated.

Silicon complexes

Our group commenced work on main group element complexes of the imidazolin-2-iminato ligand a few years ago and described its complex with a silicon(II) centre in 2012.[21] High interest for molecular low-valent silicon compounds originates from their various applications in catalysis and bond activation.[22,23] Conversion of $L^{Dip}NLi$ with $Cp^*Si[B(C_6F_5)_4]$ (Cp^* = pentamethylcyclopentadienyl) as a source of silicon(II) afforded the pentamethylcyclopentadienyl imino silylene **40** with η^2 coordination of the silicon centre by the organyl ligand (Scheme 9). An alternative synthetic route by which **40** can be accessed is *via* reaction of $L^{Dip}NLi$ with Cp^*SiBr_3 followed by reductive dehalogenation of $L^{Dip}NSi(Br_2)Cp^*$ (**41**). Unfortunately, this method affords only very poor yields of the silylene. DFT calculations on **40** show some π bonding interaction between the imino nitrogen lone pair and the unoccupied p-orbital at the silicon centre. The WBI_{SiN} of 0.80 and the Si–N bond length (1.691(5) Å) imply single bond character. Thus, multiple bond interaction as illustrated by the general canonical structures $\mathbf{B^M}$ and $\mathbf{C^M}$ (Fig. 2) cannot be concluded for **40**. A key motivation of the study was to explore potential silylene–nitrene character of complexes between a low-valent silicon atom and the imidazolin-2-iminato ligand as represented by the canonical structure $\mathbf{40^A}$ (Scheme 9). However, structural and theoretical investigation verified the imino-substituted silylene formulation **40** with no relevant silylene–nitrene character ($\mathbf{40^A}$). Conversion of **40** with tris(pentafluorophenyl)borane furnished the silylene–borane adduct **42**. It is interesting to note that the Cp^* ligand is coordinated in a η^1-mode with one σ bond to the silicon atom in sharp contrast to the precursor **40**, in which η^2-mode Si–Cp^* bonding is observed. As compared to **40** the Si–N bond length is considerably reduced to 1.605(3) Å and its WBI_{SiN} is increased to 0.90 which account for partial SiN double bond character. The C–N–Si angle of 158.7(3)° in **42** is wider than in **40** (136.6(4)°). Accordingly, the relevant 1-sila-2-aza-allene nature (*cf.* $\mathbf{B^M}$, Fig. 2) can be attributed to **42** as represented by resonance structure $\mathbf{42^A}$ (Scheme 9).

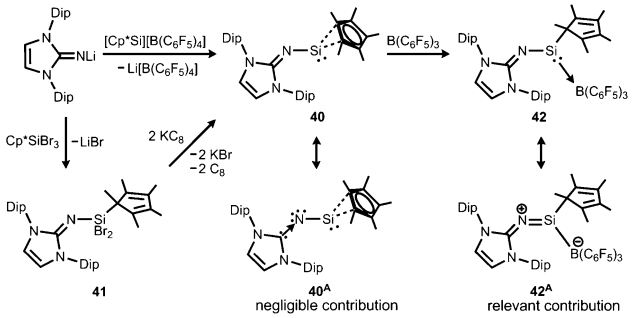

Scheme 9 Synthesis of Cp*-substituted iminosilylene **40** and its borane adduct **42**, as well as the dibromide precursor **41**. Silylene–nitrene formulation $\mathbf{40^A}$ and sila-2-aza-allene canonical structure $\mathbf{42^A}$.

In order to exploit the strongly electron-donating properties of an N-heterocyclic iminato ligand for tuning the reactivity of low-valent silicon species Rivard and coworkers attempted the synthesis of a hypothetical bisiminosilylene. Access to the bisiminodibromosilane precursor **43** is granted by conversion of $L^{Dip}NSiMe_3$ (**15**) with $SiBr_4$ in appropriate stoichiometry (Scheme 10).[24] The monoimino derivative $L^{Dip}NSiBr_3$ (**44**) is

Open Access Article. Published on 08 august 2016. Downloaded on 21.04.2026 03:42:46.
This article is licensed under a Creative Commons Attribution 3.0 Unported Licence.

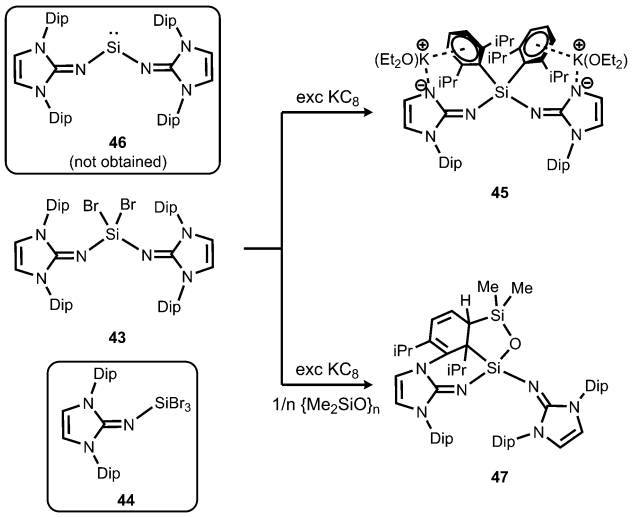

Scheme 10 Reduction of dibromosilane **43** with KC_8 to form the unexpected anionic compound **45** instead of intended **46**. The siloxane **47**, as well as the tribromide **44**.

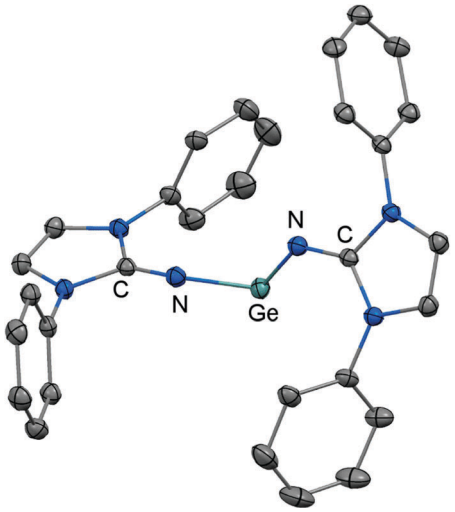

Fig. 6 Ellipsoid plot (30% level) of the bisiminogermylene **49** (hydrogen atoms and isopropyl groups have been omitted).

synthesized in a similar fashion (Scheme 10).[24] The reductive dehalogenation of **43** with KC_8 (excess) yielded the potassium salt **45** instead of the desired silylene $(L^{Dip}N)_2Si$ (**46**, Scheme 10).[24] This product (**45**) was presumed to result from an intermediate potassium silanide *via* migration of a Dip group. The formation of minor amounts of the siloxane **47** was reasoned by the presence of silicon grease in the reaction mixture (Scheme 10).

Germanium complexes

The reductive dehalogenation of the bulky bisiminodichlorogermane **48** with sodium naphthalenide affords the bisiminogermylene **49** as reported by Rivard and coworkers (Scheme 11).[24] Notably, the related monoiminotrichlorogermane **50** was also described (Scheme 11). In the solid state the germanium(II) compound (**49**) exhibits longer Ge–N distances (both: 1.8194(15) Å) and a decreased N–Ge–N bond angle (99.48(10)°) with respect to its halogenated precursor **48** (Ge–N = 1.7528(14) Å, 1.7582(14) Å; N–Ge–N = 106.33(7)°; Fig. 6). These structural features were interpreted by the authors in terms of a higher p-character of the Ge–N bond in **49** as compared to **48**. Theoretical calculations

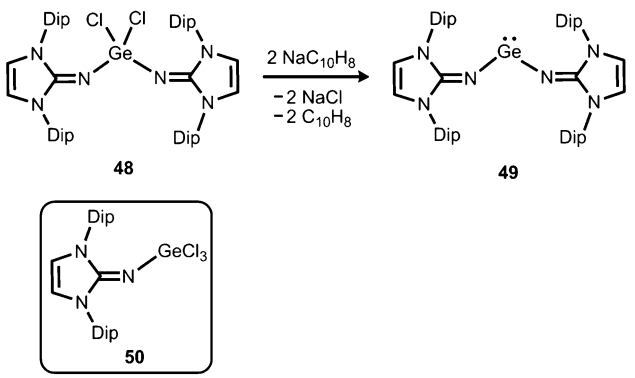

Scheme 11 Reductive dehalogenation of the dichlorogermane **48** to the bisiminogermylene **49**. The trichlorogermane **50**.

indicated a low singlet–triplet gap of 45.8 kcal mol^{-1} for the bisiminogermylene **49**, a value which is similar to that of the elusive bisiminosilylene **46** (44.5 kcal mol^{-1}). This computational study suggests high inclination for the sterically hindered metal centre to insert into element–element bonds of small substrate molecules. However, upon conversion of **49** with dihydrogen Rivard and coworkers observed the formation of $L^{Dip}NH$ as the only soluble species instead of the expected $(L^{Dip}N)_2GeH_2$.[24] This may account for the pronounced proton affinity of the imidazolin-2-imino group. Interestingly, the bisiminogermane is also not formed in the reaction of **48** with hydride transfer reagents such as $K[BHsBu_3]$ or potassium hydride.[24]

Another synthetic approach to germanium(II) complexes of the imidazolin-2-iminato ligand uses the Lappert's germylene $((Me_3Si)_2N)_2Ge$ as a low-valent metal source. Its conversion with one equiv. of $L^{Dip}NH$ at 50 °C furnishes the amino(imino)germylene **51** in the form of a viscous liquid (Scheme 12).[25] It acts as a ligand towards iron carbonyls as demonstrated by the formation of the germylene complex **52** after reaction of **51** with diironnonacarbonyl (Scheme 12).[25a] The XRD analysis of **52** reveals a $Ge–N_{imino}$ distance of 1.755(2) Å which is significantly shorter than the $Ge–N_{amino}$ bond length of 1.839(2) Å and also with respect to the free bisiminogermylene **49** (*vide supra*). Considering the WBIs of the Ge–N bonds in **52** ($Ge–N_{imino}$ = 0.86, $Ge–N_{amino}$ = 0.60) it is reasonable to assume that the bulky imidazolin-2-iminato ligand bonds stronger to the germanium(II) centre than the bis(trimethylsilyl)-amino group, presumably as a result of the iminato ligand's higher electron-donating character.

If treated with tris(pentafluorophenyl)borane compound **51** undergoes a methyl-abstraction and ring-closing reaction to form the cyclic germyliumylidene **53**$[MeB(C_6F_5)_3]$ as an example for a cationic complex of germanium(II) (Scheme 13, Fig. 7).[25a] The bonding situation in 53^+ is found to be suitably described as an amino-bonded cationic germanium(II) atom that is stabilized *via* dative bond type interaction with an intramolecularly tethered imino group. This is indicated by a weaker interaction

Open Access Article. Published on 08 august 2016. Downloaded on 21.04.2026 03:42:46.
This article is licensed under a Creative Commons Attribution 3.0 Unported Licence.

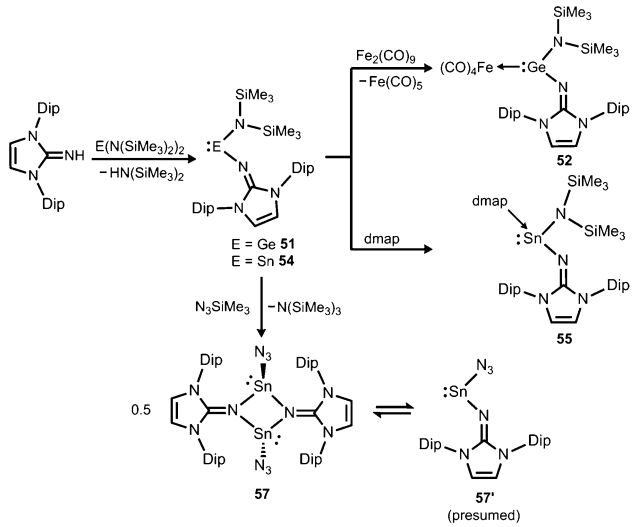

Scheme 12 Preparation of amino(imino)metallylenes **51** and **54** and the iron carbonyl **52**, as well as the dmap adduct **55** (dmap = 4-dimethylamino-pyridine). Conversion of **54** to dimeric stannylene azide **57**.

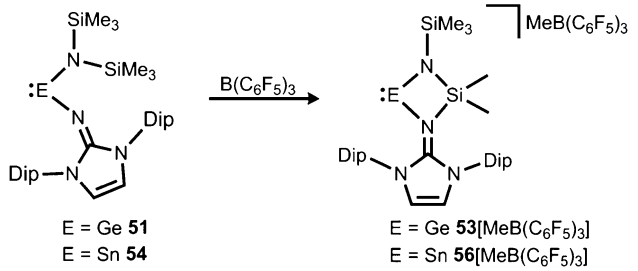

Scheme 13 Synthesis of four-membered metallyliumylidenes 53^+ and 56^+ by methyl-abstraction from the amino(imino)metallylenes **51** and **54**.

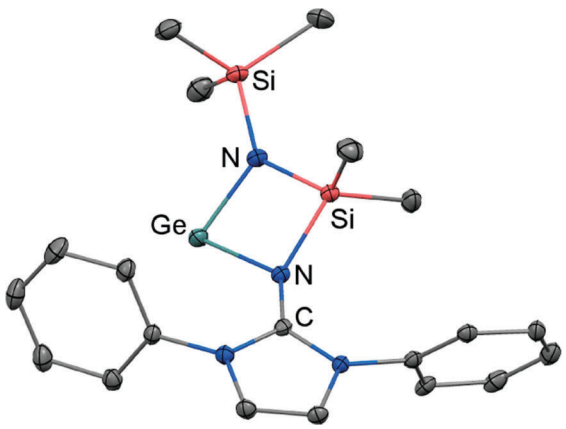

Fig. 7 Ellipsoid plot (30% level) of the germyliumylidene 53^+ (hydrogen atoms and isopropyl groups have been omitted).

between the Ge(II) centre and the N_{imino} atom (Ge–N_{imino} = 1.9694(14) Å, WBI_{GeN} = 0.48) and a stronger bond between the Ge(II) centre and the N_{amino} atom (Ge–N_{amino} = 1.8437(15) Å, WBI_{GeN} = 0.73). This bonding situation between the metal centre and the N atoms appears to be in contrast to the situation in the uncharged congeners **51** and **52** (*vide supra*). Moreover, the C–N_{imino} distance of 1.335(2) Å in 53^+ is greater in comparison to **52** (C–N_{imino} = 1.296(3) Å) and hints towards delocalization of cationic charge into the imidazoline ring system similar to the observations reported for **5**, as well as 14^+. This accounts for the pronounced ability of the imidazolin-2-iminato ligand to stabilize cationic species which was verified yet again by a very recent report on the isolation of bifunctional germylene–germyliumylidenes.[25b]

Tin complexes

In 2015 the formation of the amino(imino)stannylene **54** was reported that proceeds in a similar fashion to the lighter congener **51** *via* reaction of $((Me_3Si)_2N)_2Sn$ with $L^{Dip}NH$ at 60 °C (Scheme 12).[26] Notably, the ^{119}Sn NMR chemical shift of −208 ppm for **54** (C_6D_6) is considerably shifted to higher field with respect to the precursor (767 ppm, C_6D_6) which was accredited to an aggregated species in solution with a higher coordinate tin(II) centre. The compound (**54**) was obtained as a pale red powder and reacted with 4-dimethylamino-pyridine (dmap) to give the solid tin(II) adduct **55** that exhibited a resonance at −3 ppm in the ^{119}Sn NMR spectroscopic analysis (Scheme 12).[26] The XRD study of **55** shows a shorter Sn–N_{imino} contact (2.0588(13) Å) and a longer Sn–N_{amino} distance (2.1647(12) Å). This was interpreted in terms of a stronger bond of the metal centre to the iminato ligand and a weaker interaction with the amino group as described for the germanium congener **52**, as well (*vide supra*).[25,26] The reaction of **54** with tris(pentafluorophenyl)borane affords the stannyliumylidene salt **56**[$MeB(C_6F_5)_3$] in a methyl abstraction and ring closing reaction similar to the process that afforded the germanium analogue **53**[$MeB(C_6F_5)_3$] (Scheme 13, *vide supra*). The bonding situations in 56^+ and 53^+ resemble, that is, an amino bonded metallyliumylidene cation which is stabilized by a dative bond to the imino group. Accordingly, the Sn–N_{imino} distance of 2.197(2) Å in 56^+ is longer than the Sn–N_{amino} bond length of 2.062(2) Å which is an observation that is in contrast to that reported for the uncharged congener **55** that possesses a shorter Sn–N_{imino} contact. The isolation of **56**[$MeB(C_6F_5)_3$] is another example for the high potential of N-heterocyclic imino systems to stabilize cationic species. Interestingly, the amino-(imino)stannylene **54** converts with azido trimethylsilane to the dimeric iminostannylene azide **57** (Scheme 12).[26] Apparently, an expected stannaimine of the type $(L^{Dip}N)((Me_3Si)_2N)Sn(NSiMe_3)$ is not formed but ligand exchange results in the liberation of $(Me_3Si)_3N$ from the system. Interestingly, in solution (THF-d_8) dimeric **57** ($\delta(^{119}Sn)$ = −285 ppm) exists in equilibrium with a monomeric species ($\delta(^{119}Sn)$ = 39 ppm; **57′**, Scheme 12).

Very recently, our group described the bisiminochlorostannate **58** which forms by the reaction of $L^{Dip}NLi$ with half an equivalent of $SnCl_2$·1,4-dioxane (Scheme 14).[27] The ^{119}Sn NMR spectrum of **58** (thf-d_8) shows a resonance at −18 ppm that is shifted to a lower field in comparison to common monomeric trigonal pyramidal-coordinate 1,3-diketiminato tin(II) chlorides (−118 ppm to −337 ppm).[28] The XRD analysis of **58** reveals a butterfly-shaped four-membered SnN_2Li stannacycle with no bonding interaction

Open Access Article. Published on 08 august 2016. Downloaded on 21.04.2026 03:42:46.
This article is licensed under a Creative Commons Attribution 3.0 Unported Licence.

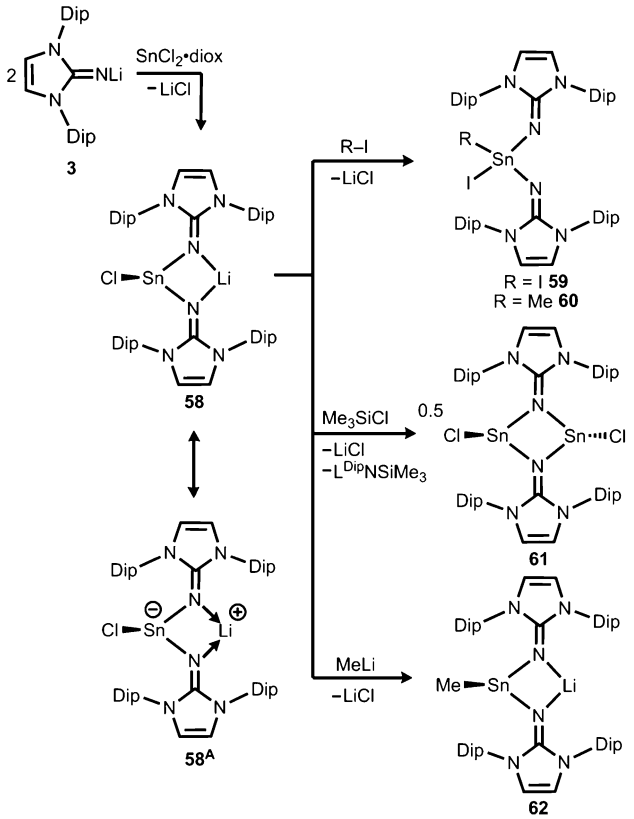

Scheme 14 Synthesis of bisiminostannylenoid **58** and reactivity with I_2, MeI, $ClSiMe_3$ and MeLi to products **59–62** (diox = 1,4-dioxane).

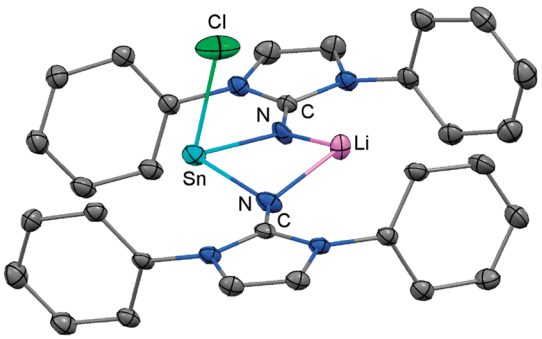

Fig. 8 Ellipsoid plot (30% level) of the stannylenoid **58** (hydrogen atoms and isopropyl groups have been omitted).

between the Sn atom and the Li atom (Fig. 8). The $Sn–N_{imino}$ distances of 2.143(5) Å and 2.179(4) Å are longer compared with that of the dmap adduct **55**. The $Li–N_{imino}$ bond lengths of 1.946(9) Å and 2.004(9) Å are comparable to those reported for the imino lithium dimer $[L^{Dip}NLi]_2$·toluene (**3**·toluene).[8]

Compound **58** reacts with electrophiles such as I_2 and MeI to form the oxidative addition products **59** and **60** which demonstrates its stannylene character. For the bulky substrate Me_3SiCl the analogous formation of the stannane $(Me_3Si)ClSn(L^{Dip})_2$ is suppressed and $L^{Dip}SiMe_3$ is formed along with the dimeric chlorostannylene $[L^{Dip}SnCl]_2$ (**61**). The bisiminochlorostannate (**58**) may also act as an electrophile. Its conversion with MeLi

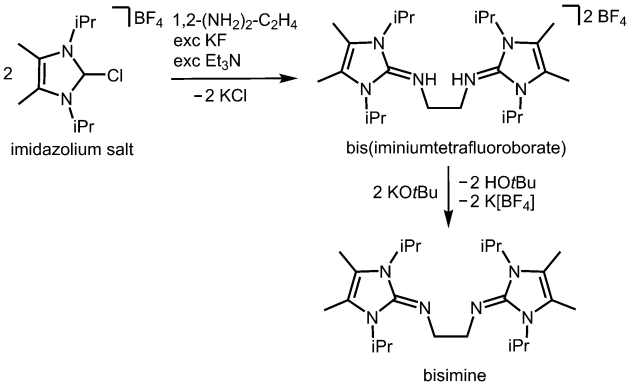

Scheme 15 Synthesis of the bisimine compound 1,2-$(L^{iPr_2Me_2}N)_2$-C_2H_4 ($L^{iPr_2Me_2}$ = 1,3-diisopropyl-4,5-dimethyl-imidazolin-2-ylidene) from an imidazolium salt precursor.

leads to the formation of Me-substituted stannate **62** that exhibited a planar four-membered LiN_2Sn ring in the XRD analysis. Theoretical calculations on **58** revealed the high single-bond character of the $Sn–N_{imino}$ interactions as concluded from the comparison of the WBI values of **58** (0.43 and 0.44) with the ones in **61** (0.24 and 0.24) which mark considerable dative-bond character for the latter. Moreover, the computational study of the natural population analysis (NPA) charge distribution in **58** and **61** shows that the Sn atom in **58** is less positively polarized (+1.22) than that in **61** (+1.42). These theoretical results account for the stannyl anion character of **58** as illustrated by the resonance structure **58**^{A} (Scheme 14). However, the ambiphilic reactivity of the tin(II) centre in **58**, that is, it functions as a nucleophile in the synthesis of **59** and **60** and as an electrophile in the conversion to **62**, has to be pointed out. It allows for the conclusion that the compound (**58**) possesses high stannylenoid character and thus represents a heavier congener of carbenoids.

Miscellaneous: survey of carbon chemistry

In the field of coordination chemistry the tethering of the exocyclic imino-nitrogen atom of an N-heterocyclic imino group to a carbon atom mostly serves the creation of tailor-made ligand systems. These synthetic methods have been reviewed elsewhere.[2,3] They can be complemented by the report of Tamm and coworkers in 2014 on the modified synthesis of the bisimine 1,2-$(L^{iPr_2Me_2}N)_2$-C_2H_4 ($L^{iPr_2Me_2}$ = 1,3-diisopropyl-4,5-dimethyl-imidazolin-2-ylidene, Scheme 15), a chelate-fashioned ligand system which had been described before in the year 2007.[29,30]

Group 15 element complexes

Background

For the pnictogen family compounds of phosphorus with the imidazolidin-2-imino group (saturated in the ligand backbone) dominate the field. As outlined in the following section this ligand system is often implemented for the stabilization of phosphorus-centred radicals and suits the requirements for the isolation of cationic species similar to the strongly related imidazolin-2-imino group (unsaturated in the ligand backbone).

 This journal is © The Royal Society of Chemistry 2016

Open Access Article. Published on 08 august 2016. Downloaded on 21.04.2026 03:42:46.
This article is licensed under a Creative Commons Attribution 3.0 Unported Licence.

Most notably, pioneering work on imidazolin-2-imino-substituted phosphanes was reported by Kuhn and coworkers in 1996 and 1998.[31] Also, compounds with the imidazolin-2-imino structural motif adjacent to a nitrogen atom are abundant. Examples include common types of organic compounds such as azines of cyclic ureas, cyclic bisguanidines, as well as triazenes and diazotates with the corresponding C_3N_2 five-membered ring backbone. These will be discussed in the miscellaneous section of this review. Interestingly, the respective chemistry of the heavier pnictogens remains largely unexplored to date.

Phosphorus compounds

Phosphorus mononitrides and phosphinonitrenes have developed into an established subgenre of the iminato ligand-stabilized phosphorus chemistry and respective research was sparked by Bertrand and coworkers in 2010. They reported the use of the imidazolidin-2-imino lithium reagent $(H_2)L^{Dip}NLi$ for the synthesis of the phosphorus dichloride **63** which undergoes reductive dehalogenation with magnesium in the presence of a cyclic alkyl(amino) carbene (CAAC) to afford **64** (Scheme 16, Fig. 9).[32] The authors demonstrated that this compound (**64**) can be regarded as a molecular congener of phosphorus mononitride stabilized by a CAAC as a ligand to the phosphorus atom and an NHC at the P-bonded nitrogen atom (**64**$^{\mathbf{A}}$, Scheme 16). This resonance structure (**64**$^{\mathbf{A}}$) is reminiscent of the diphosphorus compounds **65** and **66** that bear two NHC ligands or two CAACs, respectively (Scheme 16).[33,34]

The formulation **64** represents the phosphazabutadiene character of the compound. In the ^{31}P NMR spectroscopic analysis the chemical shift of **64** is observed at 134 ppm which is shifted to a lower field with respect to the heavier congeners **65** and **66** (range: from 59 ppm to −74 ppm). As derived from XRD analysis the geometry of **64** (Fig. 9) was described as *trans*-bent with a short P–C_{CAAC} bond (1.719(2) Å), as well as an N–C_{NHC} distance (1.282(3) Å) that is in the range of C–N bond lengths of imino groups (*vide supra*). The P–N distance of 1.7085(16) Å is similar to that of typical P–N single bonds. Oxidation of **64** with $Ph_3C[B(C_6F_5)_4]$ (trityl tetrakis(pentafluorophenyl)borate) afforded

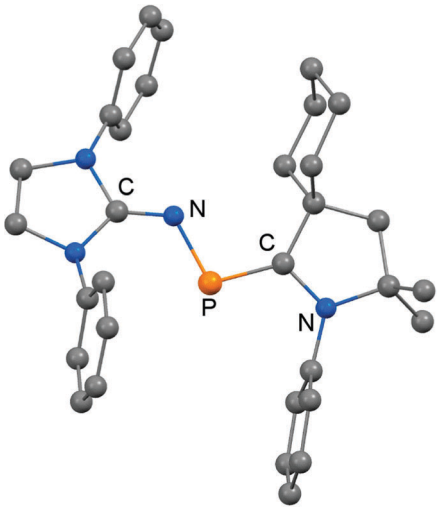

Fig. 9 Ball and stick representation of the phosphazabutadiene **64** as derived from XRD analysis (hydrogen atoms and isopropyl groups have been omitted).

the radical cation **64**$^{+\bullet}$ (Scheme 16).[32] This process is reversible as was shown by the regeneration of uncharged **64** *via* reduction with potassium graphite (KC_8, Scheme 16). In the theoretical analysis of **64** and **64**$^{+\bullet}$ the shapes of the HOMO and the SOMO (singly occupied molecular orbital), respectively, are very similar. They majorly comprise a π* orbital of the PN group that shows bonding interaction with a p-type orbital at the carbenic atom of the NHC, as well as the CAAC ligand.[32] The EPR study of **64**$^{+\bullet}$ in frozen fluorobenzene at 100 K revealed *g*-tensors of $g_x = 2.0052$, $g_y = 2.0087$ and $g_z = 2.0028$ which are comparable to the respective values in **65**$^{+\bullet}$ and **66**$^{+\bullet}$.[32–34]

The scope of applications of N-heterocyclic imines in phosphorus chemistry was extended in 2011 when Bertrand and coworkers reported the reduction of the bisimino compound **67**[OTf] (Tf = triflyl) with KC_8 to the uncharged phosphinyl radical **67**$^{\bullet}$ (Scheme 17, Fig. 10).[35] Notably, the synthesis of **67**[OTf] proceeds *via* the chloride salt **67**[Cl] that could not be isolated in analytically pure form at that time but is purified in

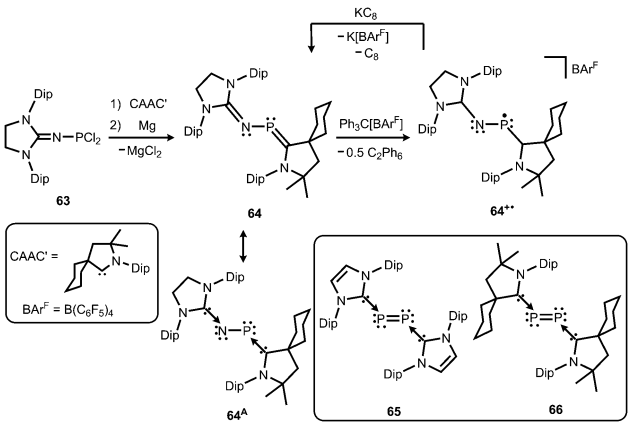

Scheme 16 Synthesis of phosphazabutadiene **64** and its conversion to the radical cation **64**$^{+\bullet}$. Phosphorus mononitride formulation **64**$^{\mathbf{A}}$. NHC- and CAAC-stabilized diphosphorus complexes **65** and **66**.

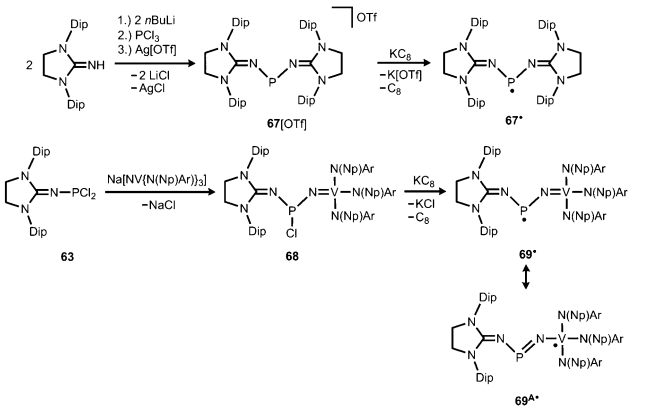

Scheme 17 Conversion of the bisiminophosphonium salt **67**[OTf] to the phosphinyl radical **67**$^{\bullet}$. Synthesis of the imino(vanadyl)phosphinyl radical **69**$^{\bullet}$ *via* chlorophosphine **68**. Vanadium-centre formulation **69**$^{\mathbf{A}\bullet}$ (Np = neopentyl).

Open Access Article. Published on 08 august 2016. Downloaded on 21.04.2026 03:42:46.
This article is licensed under a Creative Commons Attribution 3.0 Unported Licence.

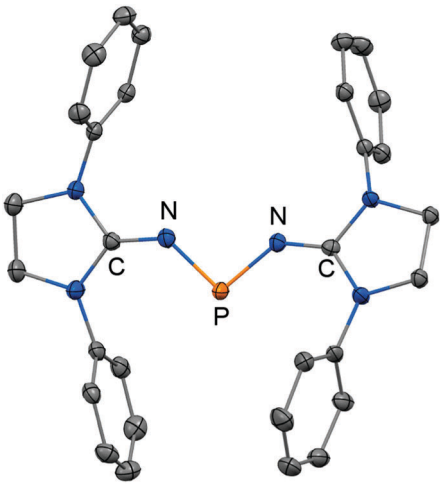

Fig. 10 Ellipsoid plot (30% level) of the bisiminophosphinyl radical **67•** (hydrogen atoms and isopropyl groups have been omitted).

the course of the anion exchange (chloride *vs.* triflate, Scheme 17).[35] The paramagnetic nature of **67•** was verified by its EPR study at 100 K in frozen THF from which the *g*-tensors g_x = 2.0074, g_y = 2.0062 and g_z = 2.0024 were derived. A comparison with hyperfine coupling constants of atomic phosphorus revealed that an unpaired electron is primarily localized on the 3p(P) orbital (62%) with a small contribution of the 3s(P) orbital (2%).

Bertrand and coworkers extended their investigation of imino-substituted phosphinyl radicals: the phosphorus dichloride **63** served as a precursor to the nitridovanadium-functionalized phosphorus monochloride **68** (Scheme 17).[35] In an analogous fashion as for **67•** the reduction of **68** with KC_8 furnished the phosphinyl radical **69•** (Scheme 17).[35] From the EPR study of **69•** *g*-tensors of g_x = 1.9726, g_y = 2.0048 and g_z = 1.9583 were determined. Taking into account the hyperfine coupling constants to ^{51}V, as well as ^{31}P it was concluded that the spin density in **69•** mainly resides on the vanadium centre (67%) and is only localized to a minor degree on the phosphorus atom and the NHC moiety. In contrast, the spin density of the bisimino derivative **67•** was found to reside with 62% in the 3p(P) orbital and with 2% in the 3s(P) orbital. In line with the structural and theoretical analysis the authors concluded that the bisimino radical **67•** is a phosphorus centred radical with little spin delocalization over the iminato ligands. The nitridovanadium congener **69•**, however, is best represented by the canonical structure **69^{A}•**, that is a vanadium(IV) complex with a phosphinimide ligand.

In 2012 Betrand and coworkers reported the remarkable transformation of the azido bisiminophosphane **70** to the phosphinonitrene species **71** *via* irradiation at 254 nm (Scheme 18).[36] As a starting material the bisiminophosphenium salt **67**[Cl] was used that had also been implemented in the synthesis of the phosphinyl radical **67•** (Scheme 17).[35,36] The theoretical analysis of the nitrene (**71**) suggested that the back donation of a nitrogen lone-pair into accessible σ* orbitals at the phosphorus atom significantly contributes to the thermodynamic

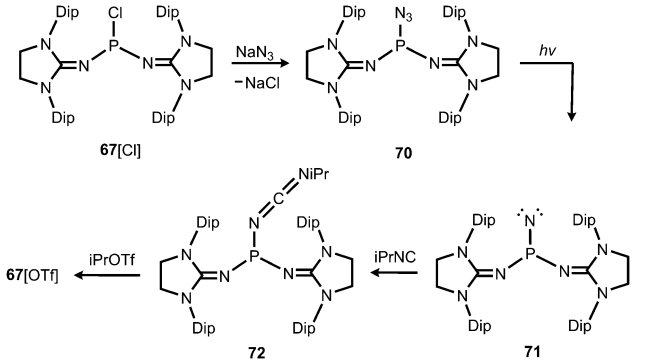

Scheme 18 Synthesis of phosphinonitrene **71** by photoirradiation of azidophosphane **70** and conversion to carbodiimide **72**.

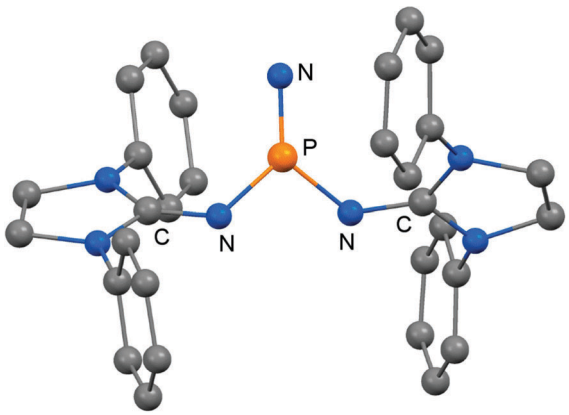

Fig. 11 Ball and stick representation of the phosphinonitrene **71** as derived from XRD analysis (hydrogen atoms and isopropyl groups have been omitted).

stability of the compound. The phosphorus atom in **71** is the centre of a trigonal-plane and the sum of the angles around the P atom amounts to 360° (Fig. 11). Notably, the P–$N_{nitrene}$ bond length of 1.457(8) Å in **71** is significantly shorter than the P–N_{imino} distances (1.618(8) Å, 1.629(8) Å), as well as the P–N_{azido} distance of 1.895(11) Å in the precursor (**70**). This is in good agreement with the upfield shift in the ^{31}P NMR spectrum of **71** (8 ppm) in comparison to **70** (111 ppm) which indicates the multiple-bond character of the PN functionality. The phosphinonitrene (**71**) reacts with isopropyl isonitrile (iPrNC) to yield the carbodiimide **72** that was not structurally characterized (Scheme 18).[36] In consequence, the created NCNiPr group can be abstracted from the phosphorus atom by implementing isopropyltriflate as an alkylating agent. In the outcome the starting material $\mathbf{67}^+$ is generated in the form of the triflate salt (**67**[OTf], Scheme 18).

Bertrand and coworkers described the transformation of the phosphinonitrene **71** to iminophosphonium triflates in 2013.[37] The methylation or protonation of **71** using methyltriflate or triflic acid, respectively, furnished **73**[OTf] or **74**[OTf] (Scheme 19). The P=N bond length of the phosphoranimine functionality in $\mathbf{74}^+$ amounts to 1.526(2) Å which is longer than the distance of these atoms in the precursor **71** (*vide supra*, note that the structural parameters of $\mathbf{73}^+$ are not discussed due to poor data quality).

 This journal is © The Royal Society of Chemistry 2016

Open Access Article. Published on 08 august 2016. Downloaded on 21.04.2026 03:42:46.
This article is licensed under a Creative Commons Attribution 3.0 Unported Licence.

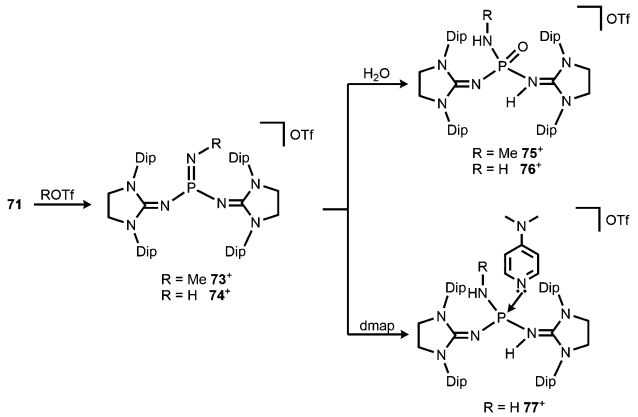

Scheme 19 Methylation and protonation of **71** to **73**[OTf] and **74**[OTf] and their reactivity towards H_2O and dmap to produce (**75–77**)[OTf].

On the other hand, the P–N_{imino} distances in $\mathbf{74}^+$ are decreased to 1.553(2) Å and 1.559(2) Å in comparison to **71** (*vide supra*). This suggests a stronger interaction between the P-centre and the imino nitrogen atoms and accounts for the potential of N-heterocyclic imino systems in stabilizing cationic species. The addition of water to **73**[OTf] or **74**[OTf] yielded the cationic phosphine oxides **75**[OTf] or **76**[OTf], respectively (Scheme 19).[37] The expected electrophilic properties of $\mathbf{74}^+$ were verified by its conversion with dmap that generated the Lewis acid base adduct **77**[OTf] (Scheme 19).[37] Notably, the ^{31}P NMR chemical shift of $\mathbf{77}^+$ was observed at a significantly higher field (−1 ppm) compared to the precursor $\mathbf{74}^+$ (73 ppm).

In 2014 the literature on the phosphinonitrene species (**71**) was enriched by Bertrand and coworkers with their investigation of coinage metal–nitrene compounds.[38] By conversion of **71** with a corresponding equivalent of copper- or silver triflate (MOTf) the respective complexes with bridging or terminal phosphinonitrene ligands are generated (**78–83**, Scheme 20). The reaction of **71** with two equiv. of MOTf furnished the bimetallic complexes **78** or **79** with a bridging nitrenic atom. These showed similar structural features in the solid state, that is, a planar coordination environment of the phosphorus atom and significantly increased P–$N_{nitrenic}$ bond lengths (1.510(5) Å for **78** and 1.528(3) Å for **79**) with respect to **71**. Furthermore, the P–N_{imino} bond lengths are shortened (1.573(3) Å for **78** and 1.561(3) Å for **79**) and, *vice versa*, the C–N_{imino} distances are lengthened (range of 1.31–1.36 Å for **78** and **79**) which indicates the stronger allocation of electron density from the imidazolidin-2-imino system to the phosphorus atom than in the precursor. After conversion of two equiv. of **71** with MOTf the linear complexes **82** and **83** with terminal bis-(phosphinonitrene) ligands were obtained.[38] Notably, the M–$N_{nitrenic}$ bond lengths (1.801(2) Å, 1.807(3) Å for **82** and 2.017(3) Å, 2.029(4) Å for **83**) in the linear complexes are decreased in comparison to the bimetallic systems (1.817(3) Å for **78** and 2.080(3) Å, 2.086(3) Å for **79**). Interestingly, the conversion of the phosphinonitrene and MOTf in a one to one ratio afforded **80** and **81**, respectively, as confirmed by NMR spectroscopic analysis. However, these compounds were found in a dynamic equilibrium with their bridging and terminal congeners (**78**, **82** for **80** and **79**, **83** for **81**).[38]

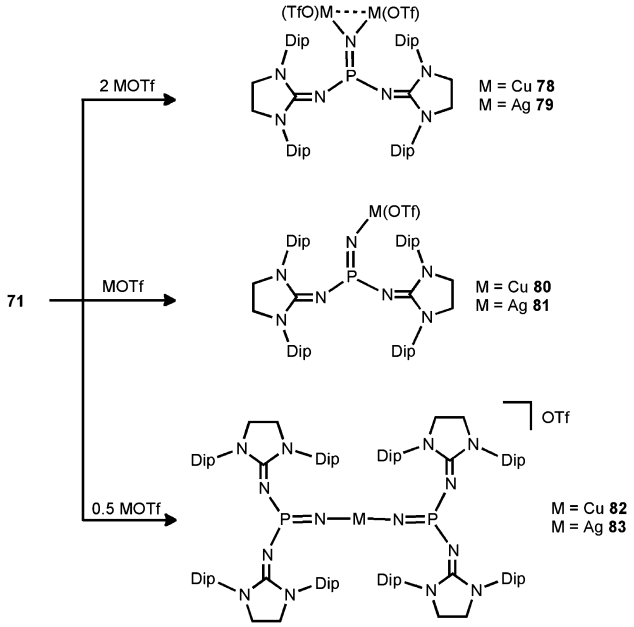

Scheme 20 The formations of metal–nitrene complexes **78–83** from phosphinonitrene **71**.

A thorough study on the reactivity of the phosphinonitrene **71** was published in 2015.[39] The authors described its thermal transformation to the iminophosphorane **84**, as well as several conversions with typical small molecule substrates (Scheme 21). At elevated temperature quantitative rearrangement of **71** was observed. The nitrenic atom inserts into a tertiary carbon CH bond of an isopropyl side chain followed by migration of the Dip moiety to the phosphorus centre to create the five membered PNC_3 ring in **84**. The addition of an excess amount of acetonitrile to the phosphinonitrene (**71**) afforded a mixture (16 : 1) of the ketenimine **85** and the diazaphosphete **86** (Scheme 21).[39] Notably, the ketenimine is transformed into the diazaphosphete at elevated temperature (90 °C). This process was reasoned by the

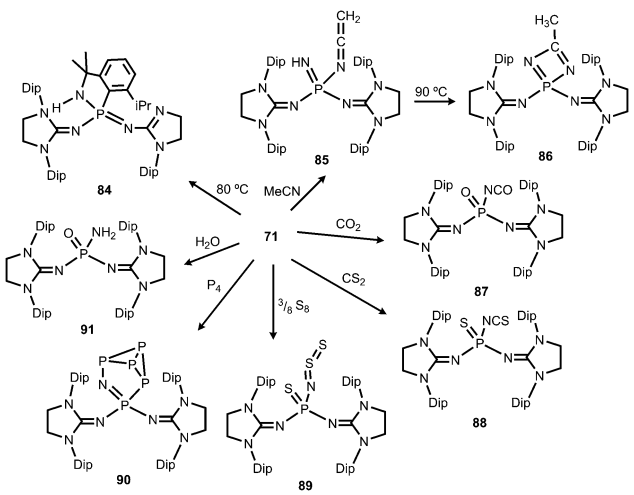

Scheme 21 Thermal conversion of phosphinonitrene **71** to **84** and reactivity with small molecules to imino complexes **85–91**.

Open Access Article. Published on 08 august 2016. Downloaded on 21.04.2026 03:42:46.
This article is licensed under a Creative Commons Attribution 3.0 Unported Licence.

initial deprotonation of acetonitrile by the nitrenic centre and nucleophilic attack of the generated cyanomethylanion at the phosphorus atom to afford **85**. Subsequent cyclization and proton migration leads to the formation of **86**. Reaction of the phosphinonitrene (**71**) with carbon dioxide or carbon disulfide yields the isocyanate **87** or the isothiocyanate **88**, respectively (Scheme 21).[39] One should point out the cleavage of the thermodynamically stable C=E double bond (E = O, S) in this process. Compound **71** activates elemental sulfur (S_8), as well as white phosphorus (P_4).[39] The reaction with S_8 furnishes the phosphine sulfide **89** that bears a thiosulfinylamino group at the phosphorus atom (Scheme 21). The conversion of **71** with P_4 affords phosphorus enriched **90** with a unique P_5N moiety *via* insertion of the $PN_{nitrene}$ fragment into a P–P single bond of the P_4 cluster (Scheme 21). With a slight excess of water the phosphinonitrene (**71**) reacted to yield the aminophosphine oxide **91** as the product of the addition of H_2O to the $PN_{nitrene}$ bond (Scheme 21).[39]

By implementing the imidazolin-2-imino trimethylsilane **92** Vidović and coworkers synthesized the imino phosphorus dichloride **93** that was reacted with carbodiphosphorane to yield the phosphenium salt **94**[Cl] (Scheme 22).[40] The latter was subjected to chloride abstraction with two equiv. of silver hexafluoroantimonate and in the outcome the dicationic phosphinimine **95**$[SbF_6]_2$ was formed (Scheme 22).[40] The dication assumes a *trans*-bent structure motif and the P–N distance of 1.594(6) Å is significantly shorter than the respective bond lengths in the CAAC congener **64** (1.7085(16) Å) and its radical cation **64**$^{+\bullet}$ (1.645(4) Å). This suggests relevant double bond character for the PN fragment in **95**$^{2+}$. As concluded from the theoretical analysis of the dication the authors attributed the increased PN interaction to the removal of electrons from the HOMO which majorly comprises the PN π^* antibonding orbital. Taking into account structural parameters such as the comparably long C–N_{imino} bond (1.367(8) Å) and bond polarizations derived from the NBO analysis it was presumed that **95**$^{2+}$ possesses dicationic phosphorus mononitride character to a minor degree (**95**$^{A2+}$, Scheme 22). Regardless of the dominant resonance structure of **95**$^{2+}$ its isolation confirms the potential of the imidazolin-2-imino ligand for stabilizing cationic species.

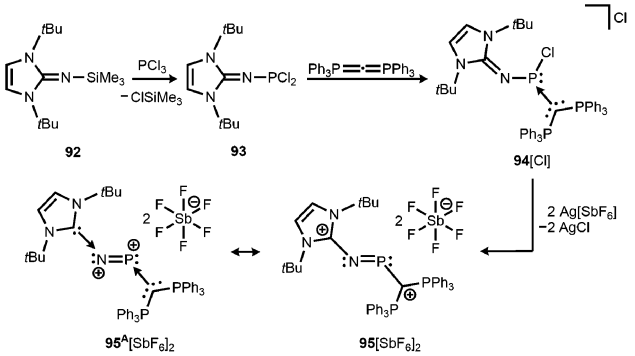

Scheme 22 Reaction of imino phosphorus dichloride to the phosphenium salt **94**[Cl] and its conversion to the dicationic phosphinimine **95**$^{2+}$. Phosphorus mononitride formulation **95**$^{A2+}$.

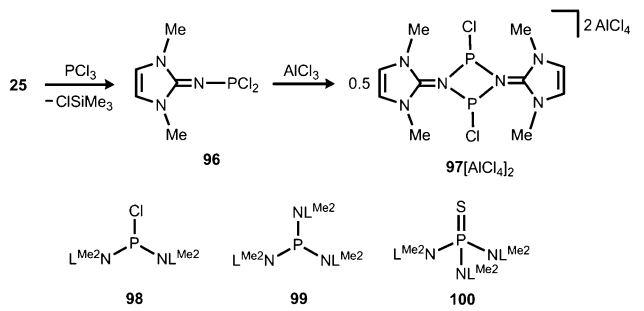

Scheme 23 Preparation of the imino phosphorus dichloride **96** from the imino trimethylsilane **25**. Reaction to the dimeric phosphenium cation **97**$^{2+}$. The iminophosphanes **98** and **99**, as well as the iminophosphorane **100**.

The application of (benz)imidazolin-2-imino substituents as supporting groups for P-based ligands has recently emerged as a subgenre of the field of phosphorus compounds of the iminato ligand. The chemistry relies on the pioneering work of Kuhn and coworkers, who converted $L^{Me_2}SiMe_3$ (**25**) to the imino dichlorophosphane **96** (Schemes 7 and 23).[31a] If treated with $AlCl_3$ this compound reacts to yield the ditopic phosphenium salt **97**$[AlCl_4]_2$, the structural formulation of which was based on NMR spectroscopic characteristics (Scheme 23).[31a] The authors described that in solution **97**$^{2+}$ is in equilibrium with **96** depending on the nucleophilic properties of the solvent. Moreover, Kuhn and coworkers described the iminophosphanes **98** and **99**, as well as the conversion of **99** to the iminophosphorane **100** (Scheme 23).[31b]

In 2015 Mallik, Panda and coworkers reported the imino diphenylphosphine **101** that was converted to the borane adduct **102**, as well as the phosphorus chalcogenides **103–106** (Scheme 24).[41]

Also in 2015 Dielmann and coworkers established the use of imidazolin-2-imino-substituted phosphines as electron-rich ligands to transition metals.[42] By lithiation of the benzimidazolin-2-imine $BL^{iPr}NH$ (**107**, BL^{iPr} = 1,3-diisopropylbenzimidazolin-2-ylidene) and reaction with the corresponding chlorophosphines the synthesis of the iminophosphines **108–113** was accomplished (Scheme 25).[42] In addition, the conversion of the bulkier $L^{Me_2Mes_2}NSiMe_3$ (**114**, $L^{Me_2Mes_2}$ = 1,3-dimesityl-4,5-dimethyl-imidazolin-2-ylidene) with the respective chlorophosphines led to the

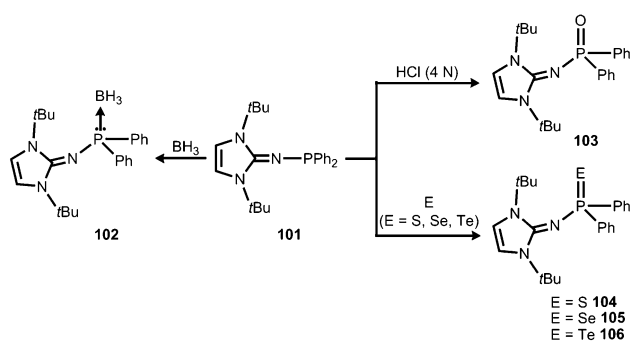

Scheme 24 Reaction of the imino diphenylphosphine **101** to the borane-adduct **102**, as well as the phosphorus chalcogenides **103–106**.

This journal is © The Royal Society of Chemistry 2016

Open Access Article. Published on 08 august 2016. Downloaded on 21.04.2026 03:42:46.
This article is licensed under a Creative Commons Attribution 3.0 Unported Licence.

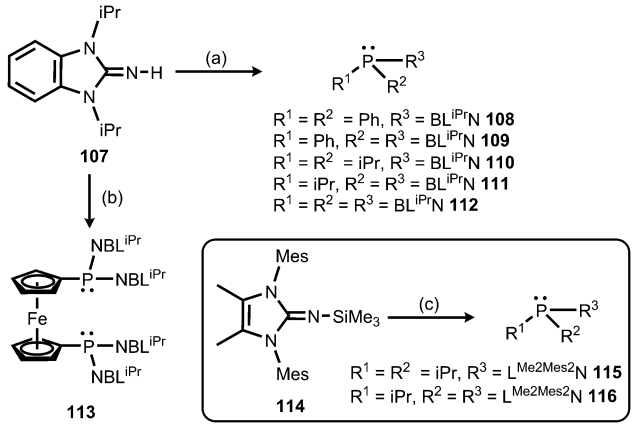

Scheme 25 Synthesis of benzimidazolin-2-imino-substituted phosphines **108–113**, as well as the imidazolin-2-imino-substituted phosphines **115** and **116**. (a) (1) *n*BuLi, THF, −78 °C; (2) chlorophosphine, room temperature. (b) (1) *n*BuLi, THF, −78 °C; (2) $[Fe(C_5H_4PCl_2)_2]$. (c) **115**: iPr_2PCl, THF; **116**: (1) PCl_3, THF, −78 °C; (2) iPrMgCl, THF, −78 °C.

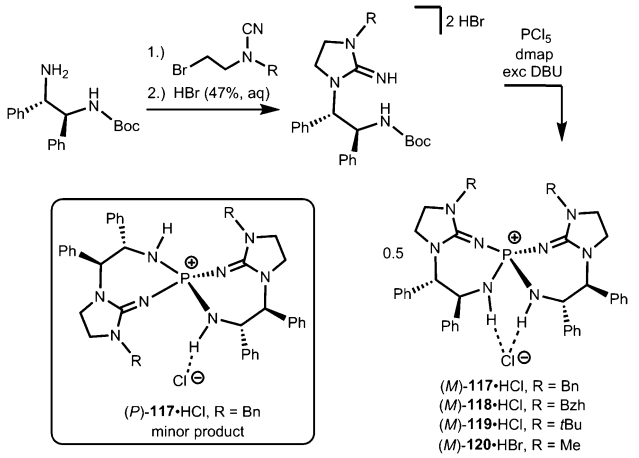

Scheme 26 Preparation of the chiral imino phosphonium halides (*M*)-**117**·HCl–(*M*)-**120**·HBr and the stereoisomer (*P*)-**117**·HCl.

iminophosphines **115** and **116** in the outcome (Scheme 25).[42] To assess the electron-donor strength of these phosphorus-based ligands the Tolman electronic parameters (TEP) of their nickel tricarbonyl complexes were determined.[43] Moreover, they were evaluated according to the Huynh's method. The ^{13}C NMR-spectroscopic shift of the carbene carbon of the BL^{iPr} group in the *trans*-{$PdBr_2(BL^{iPr})$ligand} is sensitive to the donor strength of the ligand, in which the carbene resonance of the BL^{iPr} is downfield shifted with increasing donor strength of the ligand *trans* to the BL^{iPr} group.[44] The Huynh's parameters of the iminophosphines show the same qualitative trend as the TEP analysis. As a result, many of the iminophosphines were found to be more potent electron-pair donors than most electron-rich trialkylphosphines. Remarkably, the authors concluded that the iminophosphines **111** and **112**, as well as **115** and **116**, are stronger donor ligands than classical NHCs. In addition, the bisimine **116** was presumed to be a more potent donor ligand than the very strongly electron donating abnormal NHCs exceeding the capability of monoimine **115**, as well as the bis- and the trisimine **111** and **112**. Consequently, it was reasoned that the imidazolin-2-iminato ligand is a stronger π-electron donor than the related benzimidazolin-2-iminato ligand.

Uncharged organosuperbases that comprise the imidazolidin-2-imino fragment as a chiral bis(guanidine)iminophosphorane were described by Takeda and Terada in 2013.[45] The respective iminophosphonium salts **117**·HCl, **118**·HCl, **119**·HCl and **120**·HBr were synthesized by conversion of respective aminoguanidinium halides with phosphorus pentachloride in the presence of base followed by acidic work-up (Scheme 26).[45] The stability of the iminophosphonium hydrohalide salt, and thus the high Brønsted basicity of the uncharged compounds, relies on the properties of the iminophosphorane as an electron-rich oligodentate ligand. The free base was not characterized but generated by reaction with potassium *tert*butoxide and used *in situ* for the assessment of catalytic activity in the electrophilic amination of tetralones with azodicarboxylate.[45] Notably, no particular reason for the use of the imidazolidin-2-imino group instead of acyclic guanidino functionalities was pointed out by the authors. We assume that its implementation rather follows synthetic applicability for furnishing the chiral bis(guanidine)iminophosphorane species. Notably, the scope of catalytic applications of this compound as a chiral uncharged organosuperbase was expanded in recent years.[46]

Miscellaneous: survey of related nitrogen compounds

Compounds in which the exocyclic nitrogen atom of an N-heterocyclic imino fragment bonds to another nitrogen atom are abundant in the literature but may be accounted for in the field of classical organic chemistry rather than inorganic or organometallic coordination chemistry which is the focus of this review. They can be categorized into triazenes[47] (representative example: **121**, Scheme 27), azines[18,48] (**122**, subcategory: bisguanidines, Scheme 27), as well as diazotates[49] (**123**, Scheme 28) and their azoimidazolium[50] derivatives (**124**[BPh_4], Scheme 28).

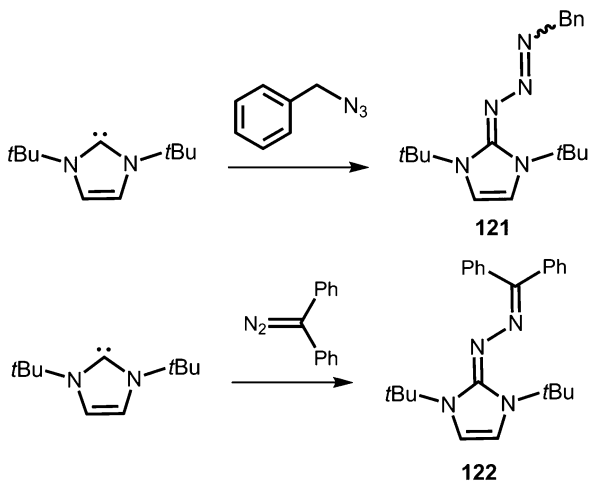

Scheme 27 Synthesis of representative examples for the compound classes: triazenes (**121**) and azines (**122**).

Open Access Article. Published on 08 august 2016. Downloaded on 21.04.2026 03:42:46.
This article is licensed under a Creative Commons Attribution 3.0 Unported Licence.

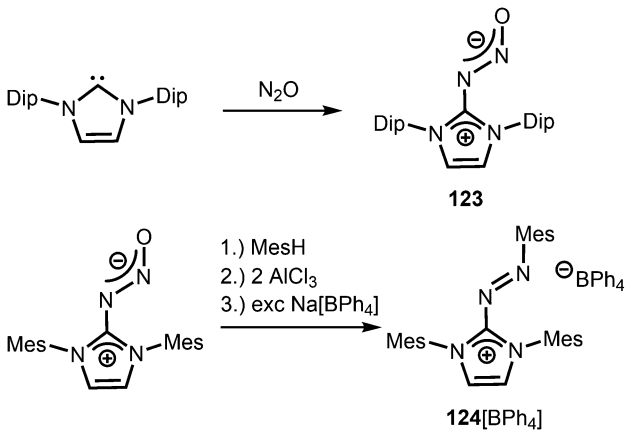

Scheme 28 Synthesis of representative examples for the compound classes: diazotates (**123**) and azoimidazolium salts (**124**[BPh_4]).

Imidazolyl triazenes (**121**) release dinitrogen under thermal conditions which leads to the formation of imino organyls whereas their exposure to acidic conditions generates a diazonium species along with the imine. The latter accounts for the pronounced proton affinity of the imidazolin-2-imino group. Apart from applications in organic chemistry azines (**122**) and diazotates (**123**), as well as their azoimidazolium spin-offs (**124**[BPh_4]), are found to be employed as ligands to main group elements or transition metals in rare instances. The mechanism for the formation of **124**[BPh_4] is proposed to involve $AlCl_3$-mediated oxygen abstraction to afford the dicationic diazonium compound, followed by its azo coupling with mesitylene. As an interesting difference in their bonding modes the C–N_{imino} distance in azines is generally shorter than in the reported diazotates. This suggests high CN double bond character for the former and considerable single bond character along with delocalization of positive charge into the imidazoline ring for the latter. Similarly, the azoimidazolium cation **124**$^+$ exhibits a comparably long C–N_{imino} bond length of 1.386(2) Å which indicates that the positive charge is majorly distributed among the atoms of the five-membered ring (Scheme 28, Fig. 12).

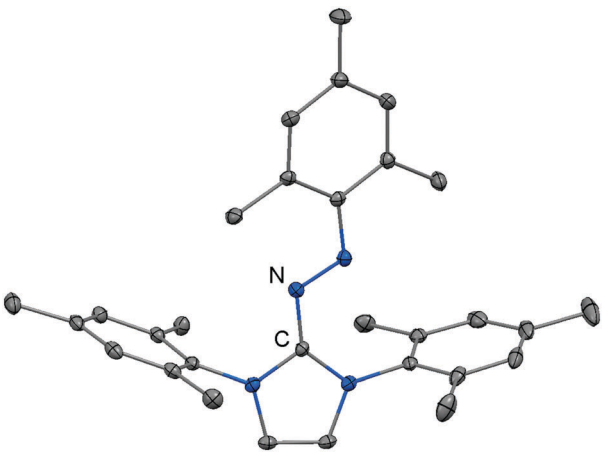

Fig. 12 Ellipsoid plot (30% level) of the azoimidazolium cation **124**$^+$ (hydrogen atoms have been omitted).

Conclusions

This survey of the coordination chemistry of main group element complexes with N-heterocyclic imines shows that these ligands are suitable for the isolation of otherwise elusive species (*e.g.* Al═Te double bond, stannylenoid, phosphinonitrene). In particular, they have proven valuable for the thermodynamic stabilization of electron-deficient central atoms, and thus enabled the isolation of rare types of low-coordinate cationic metal complexes (*e.g.* cationic thioxoborane, germyliumylidene). The strongly electron-donating character of the imidazolin-2-iminato ligand derives from the efficient delocalization of cationic charge density into the five-membered ring system. The lengthening of the C–N_{imino} distance is an indicator for the allocation of electron density by the ligand as it is often observed upon transformation of an uncharged species into a cationic offspring. The exploration of the phosphorus chemistry of this imino ligand demonstrates its applicability for the stabilization of charged, as well as uncharged phosphorus-centred radicals. Moreover, the electron-rich nature of the imidazolin-2-imino group has resulted in a new class of phosphines that bear supporting imino groups and act as highly electron donating phosphorus-centred ligands.

The chemistry of N-heterocyclic iminato complexes of main group elements is still in its infancy as compared to the widespread field of metal amides.[51] However, the growing interest in N-heterocyclic imines in recent years underlines their usefulness as ancillary ligands and distinguishes them from other classes of nitrogen-based ligand systems. Future work should study yet unexplored complexes of the imidazoli(di)n-2-imino group with heavier main group metals and focus on catalytic applications of the respective systems.

Acknowledgements

Financial support of the WACKER Chemie AG, as well as the European Research Council (SILION 637394) is gratefully acknowledged.

Notes and references

1 (*a*) N. Kuhn, H. Bohnen, J. Kreutzberg, D. Bläser and R. Boese, *J. Chem. Soc., Chem. Commun.*, 1993, 1136; (*b*) S. M. Ibrahim Al-Rafia, A. C. Malcolm, S. K. Liew, M. J. Ferguson, R. McDonald and E. Rivard, *Chem. Commun.*, 2011, **47**, 6987; (*c*) S. M. Ibrahim Al-Rafia, M. J. Ferguson and E. Rivard, *Inorg. Chem.*, 2011, **50**, 10543; (*d*) S. Kronig, P. G. Jones and M. Tamm, *Eur. J. Inorg. Chem.*, 2013, 2301; (*e*) Y. Wang, M. Y. Abraham, R. J. Gilliard, Jr., D. R. Sexton, P. Wei and G. H. Robinson, *Organometallics*, 2013, **32**, 6639.

2 N. Kuhn, M. Göhner, M. Grathwohl, J. Wiethoff, G. Frenking and Y. Chen, *Z. Anorg. Allg. Chem.*, 2003, **629**, 793.

3 (*a*) A. G. Trambitas, T. K. Panda and M. Tamm, *Z. Anorg. Allg. Chem.*, 2010, **636**, 2156; (*b*) Y. Wu and M. Tamm, *Coord. Chem. Rev.*, 2014, **260**, 116.

4 N. Kuhn, R. Fawzi, M. Steimann, J. Wiethoff, D. Bläser and R. Boese, *Z. Naturforsch.*, 1995, **50b**, 1779.

Open Access Article. Published on 08 august 2016. Downloaded on 21.04.2026 03:42:46.
This article is licensed under a Creative Commons Attribution 3.0 Unported Licence.

5 N. Kuhn, U. Abram, C. Maichle-Mößmer and J. Wiethoff, *Z. Anorg. Allg. Chem.*, 1997, **623**, 1121.
6 N. Kuhn, R. Fawzi, M. Steimann, J. Wiethoff and G. Henkel, *Z. Anorg. Allg. Chem.*, 1997, **623**, 1577.
7 N. Kuhn, R. Fawzi, M. Steimann and J. Wiethoff, *Z. Anorg. Allg. Chem.*, 1997, **623**, 554.
8 D. Franz, E. Irran and S. Inoue, *Dalton Trans.*, 2014, **43**, 4451.
9 D. Franz and S. Inoue, *Chem. – Asian J.*, 2014, **9**, 2083.
10 D. Franz, E. Irran and S. Inoue, *Angew. Chem., Int. Ed.*, 2014, **53**, 14264.
11 (*a*) K. Dehnicke and F. Weller, *Coord. Chem. Rev.*, 1997, **158**, 103; (*b*) S. Courtenay, J. Y. Mutus, R. W. Schurko and D. W. Stephan, *Angew. Chem., Int. Ed.*, 2002, **41**, 498; (*c*) S. Courtenay, D. Walsh, S. Hawkeswood, P. Wei, A. K. Das and D. W. Stephan, *Inorg. Chem.*, 2007, **46**, 3623; (*d*) O. Alhomaidan, E. Hollink and D. W. Stephan, *Organometallics*, 2007, **26**, 3041; (*e*) M. H. Holthausen, I. Mallov and D. W. Stephan, *Dalton Trans.*, 2014, **43**, 15201; (*f*) K. Spannhoff, R. Rojas, R. Fröhlich, G. Kehr and E. Erker, *Organometallics*, 2011, **30**, 2377; (*g*) K. Jaiswal, B. Prashanth, S. Ravi, K. R. Shamasundar and S. Singh, *Dalton Trans.*, 2015, **44**, 15779.
12 (*a*) C. M. Ong, P. McKarns and D. W. Stephan, *Organometallics*, 1999, **18**, 4197; (*b*) K. Aparna, R. McDonald, M. Ferguson and R. G. Cavell, *Organometallics*, 1999, **18**, 4241; (*c*) Z.-X. Wang and Y.-X. Li, *Organometallics*, 2003, **22**, 4900; (*d*) J. Guo, J.-S. Lee, M.-C. Foo, K.-C. Lau, H.-W. Xi, K. H. Lim and C.-W. So, *Organometallics*, 2010, **29**, 939; (*e*) C. V. Cárdenas, M. Á. M. Hernández and J.-M. Grévy, *Dalton Trans.*, 2010, **39**, 6441.
13 S. M. I. Al-Rafia, R. McDonald, M. J. Ferguson and E. Rivard, *Chem. – Eur. J.*, 2012, **18**, 13810.
14 M. W. Lui, N. R. Paisley, R. McDonald, M. J. Ferguson and E. Rivard, *Chem. – Eur. J.*, 2016, **22**, 2134.
15 Z. Yang, M. Zhong, X. Ma, S. De, C. Anusha, P. Parameswaran and H. W. Roesky, *Angew. Chem., Int. Ed.*, 2015, **54**, 10225.
16 D. Franz and S. Inoue, *Chem. – Eur. J.*, 2014, **20**, 10645.
17 (*a*) D. Franz, T. Szilvási, E. Irran and S. Inoue, *Nat. Commun.*, 2015, **6**, 10037; (*b*) D. Franz and S. Inoue, *Dalton Trans.*, 2016, **45**, 9385.
18 J. M. Hopkins, M. Bowdridge, K. N. Robertson, T. S. Cameron, H. A. Jenkins and J. A. C. Clyburne, *J. Org. Chem.*, 2001, **66**, 5713.
19 (*a*) M. Tamm, S. Randoll, T. Bannenberg and E. Herdtweck, *Chem. Commun.*, 2004, 876; (*b*) M. Tamm, D. Petrovic, S. Randoll, S. Beer, T. Bannenberg, P. G. Jones and J. Grunenberg, *Org. Biomol. Chem.*, 2007, **5**, 523.
20 S. Randoll, P. G. Jones and M. Tamm, *Organometallics*, 2008, **27**, 3232.
21 S. Inoue and K. Leszczyńska, *Angew. Chem., Int. Ed.*, 2012, **51**, 8589.
22 M. Asay, C. Jones and M. Driess, *Chem. Rev.*, 2011, **111**, 354.
23 G.-H. Lee, R. West and T. Müller, *J. Am. Chem. Soc.*, 2003, **125**, 8114.
24 M. W. Lui, C. Merten, M. J. Ferguson, R. McDonald, Y. Xu and E. Rivard, *Inorg. Chem.*, 2015, **54**, 2040.
25 (*a*) T. Ochiai, D. Franz, X.-N. Wu and S. Inoue, *Dalton Trans.*, 2015, **44**, 10952; (*b*) T. Ochiai, T. Szilvási, D. Franz, E. Irran and S. Inoue, *Angew. Chem., Int. Ed.*, 2016, DOI: 10.1002/anie.201605636.
26 (*a*) T. Ochiai, D. Franz, E. Irran and S. Inoue, *Chem. – Eur. J.*, 2015, **21**, 6704; (*b*) T. Ochiai and S. Inoue, *Phosphorus, Sulfur Silicon Relat. Elem.*, 2016, **191**, 624.
27 T. Ochiai, D. Franz, X.-N. Wu, E. Irran and S. Inoue, *Angew. Chem., Int. Ed.*, 2016, **55**, 6983.
28 (*a*) A. Akkari, J. J. Byrne, I. Saur, G. Rima, H. Gornitzka and J. Barrau, *J. Organomet. Chem.*, 2001, **622**, 190; (*b*) Y. Ding, H. W. Roesky, M. Noltemeyer, H.-G. Schmidt and P. P. Power, *Organometallics*, 2001, **20**, 1190; (*c*) P. B. Hitchcock, J. Hu, M. F. Lappert and J. R. Severn, *Dalton Trans.*, 2004, 4193; (*d*) A. P. Dove, V. C. Gibson, E. L. Marshall, H. S. Rzepa, A. J. P. White and D. J. Williams, *J. Am. Chem. Soc.*, 2006, **128**, 9834; (*e*) S. L. Choong, C. Schenk, A. Stasch, D. Dange and C. Jones, *Chem. Commun.*, 2012, **48**, 2504; (*f*) R. Olejník, Z. Padělková, R. Mundil, J. Merna and A. Růžička, *Appl. Organomet. Chem.*, 2014, **28**, 405.
29 J. Volbeda, P. G. Jones and M. Tamm, *Inorg. Chim. Acta*, 2014, **422**, 158.
30 D. Petrovic, T. Glöge, T. Bannenberg, C. G. Hrib, S. Randoll, P. G. Jones and M. Tamm, *Eur. J. Inorg. Chem.*, 2007, 3472.
31 (*a*) N. Kuhn, R. Fawzi, M. Steimann and J. Wiethoff, *Chem. Ber.*, 1996, **129**, 479; (*b*) N. Kuhn, H. Kotowski and J. Wiethoff, *Phosphorus, Sulfur Silicon Relat. Elem.*, 1998, **133**, 237.
32 R. Kinjo, B. Donnadieu and G. Bertrand, *Angew. Chem., Int. Ed.*, 2010, **49**, 5930.
33 Y. Wang, Y. Xie, P. Wie, R. B. King, H. F. Schaefer, III, P. v. R. Schleyer and G. H. Robinson, *J. Am. Chem. Soc.*, 2008, **130**, 14970.
34 O. Back, B. Donnadieu, P. Parameswaran, G. Frenking and G. Bertrand, *Nat. Chem.*, 2010, **2**, 369.
35 O. Back, B. Donnadieu, M. v. Hopffgarten, S. Klein, R. Tonner, G. Frenking and G. Bertrand, *Chem. Sci.*, 2011, **2**, 858.
36 F. Dielmann, O. Back, M. Henry-Ellinger, P. Jerabek, G. Frenking and G. Bertrand, *Science*, 2012, **337**, 1526.
37 F. Dielmann, C. E. Moore, A. Rheingold and G. Bertrand, *J. Am. Chem. Soc.*, 2013, **135**, 14071.
38 F. Dielmann, D. M. Andrada, G. Frenking and G. Bertrand, *J. Am. Chem. Soc.*, 2014, **136**, 3800.
39 F. Dielmann and G. Bertrand, *Chem. – Eur. J.*, 2015, **21**, 191.
40 Y. K. Loh, C. Gurnani, R. Ganguly and D. Vidović, *Inorg. Chem.*, 2015, **54**, 3087.
41 K. Naktode, S. D. Gupta, A. Kundu, S. K. Jana, H. P. Nayek, B. S. Mallik and T. K. Panda, *Aust. J. Chem.*, 2015, **68**, 127.
42 M. A. Wünsche, P. Mehlmann, T. Witteler, F. Buß, P. Rathmann and F. Dielmann, *Angew. Chem., Int. Ed.*, 2015, **54**, 11857.
43 C. A. Tolman, *Chem. Rev.*, 1977, **77**, 313.
44 H. V. Huynh, Y. Han, R. Jothibasu and J. A. Yang, *Organometallics*, 2009, **28**, 5395.
45 T. Takeda and M. Terada, *J. Am. Chem. Soc.*, 2013, **135**, 15306.

Open Access Article. Published on 08 august 2016. Downloaded on 21.04.2026 03:42:46.
This article is licensed under a Creative Commons Attribution 3.0 Unported Licence.

46 (*a*) T. Takeda and M. Terada, *Aust. J. Chem.*, 2014, **67**, 1124; (*b*) A. Kondoh, M. Oishi, T. Takeda and M. Terada, *Angew. Chem., Int. Ed.*, 2015, **54**, 15836; (*c*) T. Takeda, A. Kondoh and M. Terada, *Angew. Chem., Int. Ed.*, 2016, **55**, 4734.

47 (*a*) D. M. Khramov and C. W. Bielawski, *Chem. Commun.*, 2005, 4958; (*b*) D. M. Khramov and C. W. Bielawski, *J. Org. Chem.*, 2007, **72**, 9407; (*c*) D. J. Coady, D. M. Khramov, B. C. Norris, A. G. Tennyson and C. W. Bielawsky, *Angew. Chem., Int. Ed.*, 2009, **48**, 5187; (*d*) A. G. Tennyson, D. M. Khramov, C. D. Varnado Jr., P. T. Creswell, J. W. Kamplain, V. M. Lynch and C. W. Bielawski, *Organometallics*, 2009, **28**, 5142; (*e*) A. G. Tennyson, E. J. Moorhead, B. L. Madison, J. A. V. Er, V. M. Lynch and C. W. Bielawski, *Eur. J. Org. Chem.*, 2010, 6277; (*f*) R. J. Ono, Y. Suzuki, D. M. Khramov, M. Ueda, J. L. Sessler and C. W. Bielawski, *J. Org. Chem.*, 2011, **76**, 3239; (*g*) D. Jishkariani, C. D. Hall, A. Demircan, B. J. Tomlin, P. J. Steel and A. R. Katritzky, *J. Org. Chem.*, 2013, **78**, 3349; (*h*) S. Patil, K. White and A. Bugarin, *Tetrahedron Lett.*, 2014, **55**, 4826; (*i*) F. W. Kimani and J. C. Jewett, *Angew. Chem., Int. Ed.*, 2015, **54**, 4051.

48 (*a*) B. Bildstein, M. Malaun, H. Kopacka, K.-H. Ongania and K. Wurst, *J. Organomet. Chem.*, 1999, **572**, 177; (*b*) M. Reinmuth, C. Neuhäuser, P. Walter, M. Enders, E. Kaifer and H.-J. Himmel, *Eur. J. Inorg. Chem.*, 2011, 83; (*c*) J. Tauchman, K. Hladíková, F. Uhlík, I. Císařová and P. Štěpnička, *New J. Chem.*, 2013, **37**, 2019; (*d*) H. Herrmann, M. Reinmuth, S. Wiesner, O. Hübner, E. Kaifer, H. Wadepohl and H.-J. Himmel, *Eur. J. Inorg. Chem.*, 2015, 2345.

49 (*a*) A. G. Tskhovrebov, E. Solari, M. D. Wodrich, R. Scopelliti and K. Severin, *Angew. Chem., Int. Ed.*, 2012, **51**, 232; (*b*) A. G. Tskhovrebov, E. Solari, M. D. Wodrich, R. Scopelliti and K. Severin, *J. Am. Chem. Soc.*, 2012, **134**, 1471; (*c*) A. G. Tskhovrebov, B. Vuichoud, E. Solari, R. Scopelliti and K. Severin, *J. Am. Chem. Soc.*, 2013, **135**, 9486.

50 A. G. Tskhovrebov, L. C. E. Naested, E. Solari, R. Scopelliti and K. Severin, *Angew. Chem., Int. Ed.*, 2015, **54**, 1289.

51 (*a*) M. F. Lappert, P. P. Power, A. V. Protchenko and A. L. Seeber, *Metal Amide Chemistry*, Wiley-VCH, Weinheim, 2009; (*b*) D. L. Kays, *Chem. Soc. Rev.*, 2016, **45**, 1004.

 This journal is © The Royal Society of Chemistry 2016